Structures 32 (2021) 1734–1751

Contents lists available at ScienceDirect

Structures

journal homepage: www.elsevier.com/locate/structures

Shear behavior of RC beams reinforced with internal trussed steel strips at shear span zone

Emad E. Etman [a], Hamdy M. Afefy [a,b,*], Ahmed T. Baraghith [a], Mohammed Abuelwafa [b]

[a] Department of Structural Engineering, Faculty of Engineering, Tanta University, Tanta, Egypt
[b] Construction Engineering and Management Department, Faculty of Engineering, Pharos University, Alexandria, Egypt

ARTICLE INFO

Keywords:
Shear behavior
Trussed steel assembly
Experimental test
Shear crack width
Reinforced concrete beams

ABSTRACT

This paper presents an experimental study on the shear performance of reinforced concrete (RC) beams provided with pre-prepared steel trusses in the shear span zone. Those steel trusses were assembled using electrical welding for steel strips of 2 mm thickness. For comparison purpose, corresponding steel trusses were assembled from equivalent rounded steel bars and used to reinforce the shear span zone of corresponding reinforced concrete beams, and then the shear behavior of beams reinforced with either trussed strips or trussed bars was compared. Accordingly, an experimental program consisted of fifteen reinforced concrete beams included one control beam have been prepared where the shear span-to-depth ratio was the same for all beams (2.3). Experimental test results showed that the beams reinforced with trussed steel strips showed better shear performance from the viewpoint of both the ultimate capacity and the developed major shear crack width compared with those of the beams reinforced with equivalent trussed bars. That is because the internal trussed strips have higher surface area than that of the equivalent rounded bars, which enabled the reinforced beam to maintain the confinement of the concrete core inside the section thus decreased the major shear crack width and increased the ultimate strength of reinforced concrete beam. Consequently, the ultimate capacity for reinforced concrete beams reinforced with internal trussed strips was higher than the corresponding capacity of beams reinforced with equivalent trussed bars by an average value of about 16%. Besides, the internal steel strips hindered the appearance of shear cracks and decreased the major shear crack width compared to the case of using equivalent rounded bars. Moreover, the experimental findings showed comparable results against the available analytical models from the viewpoints of ultimate shear capacity and maximum shear crack width.

1. Introduction

Shear failure of reinforced concrete beam is brittle and characterized by unpredictable nature after the initiation of diagonal cracks owing to the debilitated tensile resistance of concrete [1], which jeopardizes both reinforced concrete structure and the human lives. That makes shear failure more critical than flexural one for the same beam. Besides, shear cracks are documented to propagate at a faster rate compared with the flexural ones [2]. Therefore, it is important to avoid the occurrence of such failure. For this reason, it is obviously necessary to improve the shear performance and the ultimate shear strength of reinforced concrete beams for civil engineering structures, and also to keep the shear crack width within the acceptable range [2].

The shearing force in reinforced concrete beams is resisted by the uncracked concrete chord (compression chord or cantilever action), the friction forces developed along the crack length (aggregate interlock), the shear strength provided by the longitudinal reinforcement (dowel action), the residual tensile stresses of concrete and the transverse reinforcement. Consequently, it is usually accepted that the shear strength in reinforced concrete beam is provided by several contributing actions, whose relative contribution changes as the load increases and the developed shear cracks open and propagate [3–13].

In order to enhance the shear resistance of reinforced concrete beams, there are two approaches. The first one is based on enhancing the inherent tensile characteristics and thus shear strength of the used concrete using high-strength concrete [3,14] or high-performance concrete provided with internal short fibers [15–29]. The second approach is based on providing special web reinforcement in order to increase the

* Corresponding author at: Construction Engineering and Management Dept., Faculty of Engineering, Pharos University, Alexandria, On leave from Tanta University, Egypt.
E-mail addresses: hamdy.afefy@pua.edu.eg, hamdy.afefy@f-eng.tanta.edu.eg (H.M. Afefy).

https://doi.org/10.1016/j.istruc.2021.03.093
Received 20 July 2020; Received in revised form 9 December 2020; Accepted 19 March 2021
Available online 15 April 2021
2352-0124/© 2021 Institution of Structural Engineers. Published by Elsevier Ltd. All rights reserved.

contribution of the transverse reinforcement.

At the design stage, reinforced concrete beams entail web shear reinforcement in the shape of vertical stirrups, inclined stirrups, or bent up bars in order to resist the shear stresses under the worst case scenario of the applied loads when the concrete shear strength is exceeded [2,30,31]. Several alternatives to the traditional configurations of web reinforcement were investigated for shear strength enhancement such as additional horizontal and independent bent-up bars [32], welded swimmer bars, bolted swimmer bars, and u-link bolted swimmer bars [33,34], space swimmer bars [35], vertical steel plates [36] and spiral stirrups [37].

Besides, other researchers studied partially reinforced concrete structures consisting of prefabricated steel trusses embedded in cast-in-place concrete beams, where the embedded steel truss run along the entire span of the beam [38–44]. For this system, prefabricated steel trusses can sustain their own weight as well as the weight of fresh concrete without any provisional support and named as un-propped structures [45]. After hardening of concrete, the internal steel trusses work together with the cast-in-place concrete for resisting the applied loads. However, partially prefabricated structures are used to create composite steel and concrete beams (CSCB) to resist both bending moment and shearing force making use of the tensile and compressive resistances of the upper and lower chords as well as the internal members of the steel truss [46]. In spite of the favorable characteristics of such system, there are no specific guidelines for design and configurations for this type of reinforced concrete beam stipulated in design codes of practice. However, the uses of both numerical and analytical models assist in obtaining a comprehensive overview on the behavior of concrete beams reinforced with embedded steel trusses [42,47–51]. In addition, composite beams constructed from concrete-encased steel truss welded to a continuous steel plate are proposed and analyzed numerically [51].

For some instances, the flexural capacity of the beam is fulfilled; however, the shear resistance has to be upgraded to withstand the applied load. Therefore, providing embedded prefabricated steel truss in the shear span zone is required to enhance the shear resistance of the beam in comparison with traditional stirrups. Besides, the required embedded steel truss has to be composed of steel members able to restrain the propagation of the major shear cracks approaching failure. Hence, the reinforced concrete beam provided with such embedded steel truss could sustain higher acting load accompanied with narrower major shear crack width compared with reinforced concrete beam reinforced with traditional steel stirrups. Accordingly, in the current paper, different configurations of internal steel trusses made of thin steel plates of 2 mm thickness were assembled using electrical welding, configured and used as internal shear reinforcement for reinforced concrete beams. The main studied parameters were the configuration of truss members (vertical only, inclined only and both vertical and inclined members), the cross-sectional area of trussed members (28, 50 and 80 mm^2) and the spacing between vertical members (160, 200 and 265 mm). For all tested beams, the shear span-to-depth ratio was kept the same to be 2.3. The main comparison criteria were the ultimate shear capacity and the cracking characteristics for reinforced concrete beams reinforced with trussed steel strips in the shear span zone. For comparison purpose, the shear behavior of reinforced concrete beams reinforced with internal trussed steel strips was compared with the corresponding behavior of reinforced concrete beams reinforced with equivalent steel trusses made of rounded steel bars.

2. Experimental program

2.1. Test specimens

The experimental work program consisted of fifteen reinforced concrete beams divided into seven groups. The first group contained only one control beam without any web shear reinforcement at the left shear span, while the right shear span was reinforced with properly designed vertical stirrups of smooth bars having 8 mm diameter and spaced every 50 mm along the entire shear span as depicted in Fig. 1. That is to eliminate any shear failure at the right shear span zone even after strengthening the left shear span. The total length of the beam was 2200 mm while the center-to-center span was 2000 mm. the cross-sectional dimensions were 200 mm width by 400 mm total depth. The beam was loaded by two concentrated loads at 400 mm apart leading to shear span length of 800 mm. The beam's longitudinal reinforcement consisted of six deformed steel bars of 18 mm diameter in the tension side and 2 deformed steel bars of 16 mm diameter in the compression side. This longitudinal reinforcement was chosen in order to increase the flexural capacity of the beam more than its shear capacity. Thus, the shear span-to-depth ratio (a/d) was 2.3 in order to assure the shear failure of all beams. The concrete dimensions as well as the longitudinal and the transverse steel reinforcement for the control beam were the same for all remaining beams reinforced with internal steel trusses.

The second group consisted of three beams reinforced in the left shear span by pre-prepared steel trusses composed of steel strips of 2 mm thickness and 25 mm width arranged in vertical, inclined at 60° with the horizontal [31] and truss configurations spaced at 200 mm at depicted in Fig. 2(a-c). That is to study the effect of truss configuration. The third group consisted of three configurations identical to those of group 2, except that the truss members composed of equivalent smooth bars of 8 mm diameter as depicted in Fig. 2(d-f). The used smooth bars in all beams of group 3 had the same cross-sectional area of that used for the steel strips of group 2. That is to compare the behavior of beams reinforced with trussed strips with that of beams reinforced with equivalent trussed rounded bars.

Group 4 consisted of two beams reinforced with trussed strips of 14 and 40 mm width, respectively, while the thickness was kept constant as 2 mm (refer to Fig. 3(a, b). That is to study the effect of cross-sectional area of the used strips. Group 5 consisted of the two beams reinforced with trussed bars having equivalent cross-sectional area of the used strips in group 4. Thus, the used bar diameters for truss members of the two beams of group 5 were 6 and 10 mm, respectively as depicted in Fig. 3(c, d). The spacing between vertical members for steel trusses of all beams of groups 4 and 5 was 200 mm.

The objectives of the remaining groups (6 and 7) were to study the effect of spacing between vertical members where two different spacing were used; 160 and 265 mm, respectively, for both trussed strips of 25 mm width by 2 mm thickness and the corresponding trussed bars of 8 mm diameter as depicted in Fig. 4. The inclination angles of the inclined bars corresponding to spacing 160 and 265 mm were about 65° and 53°, respectively. Table 1 summarizes the characteristic of all beams included in the test matrix.

It is worth mentioning that all trusses were assembled using continuous electrical welding at all truss' joints. E6013 mild steel electrodes having 3 mm diameter have been used in welding process. In order to hold the two trusses at both sides of the beam at the required distance, two closed stirrups of 8 mm smooth bar diameter were welded at the upper and lower sides of the trusses as depicted in Fig. 5.

For all reinforced beams of groups 2 to 7, the lower longitudinal reinforcement were first arranged in the formworks, and then the pre-prepared trusses (refer to Fig. 5) assembled using electrical welding were installed. After that the upper longitudinal steel were placed and supported on the upper collar closed stirrup holding the trusses. Finally, the ordinary stirrups were installed and arranged. Then the steel cage for each beam was tied properly and accommodated with the assigned strain gauges at pre-selected locations.

2.2. Material properties

For the current paper, in order to have the same concrete properties for all beams as well as to control the quality of the used concrete, ready-mix concrete was used to cast all test beams at the same time. According

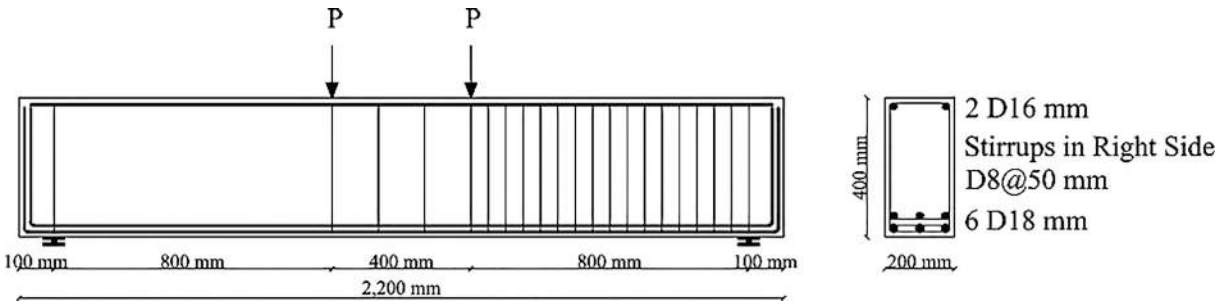


Fig. 1. Typical concrete dimensions and reinforcement detailing for control beam BC.

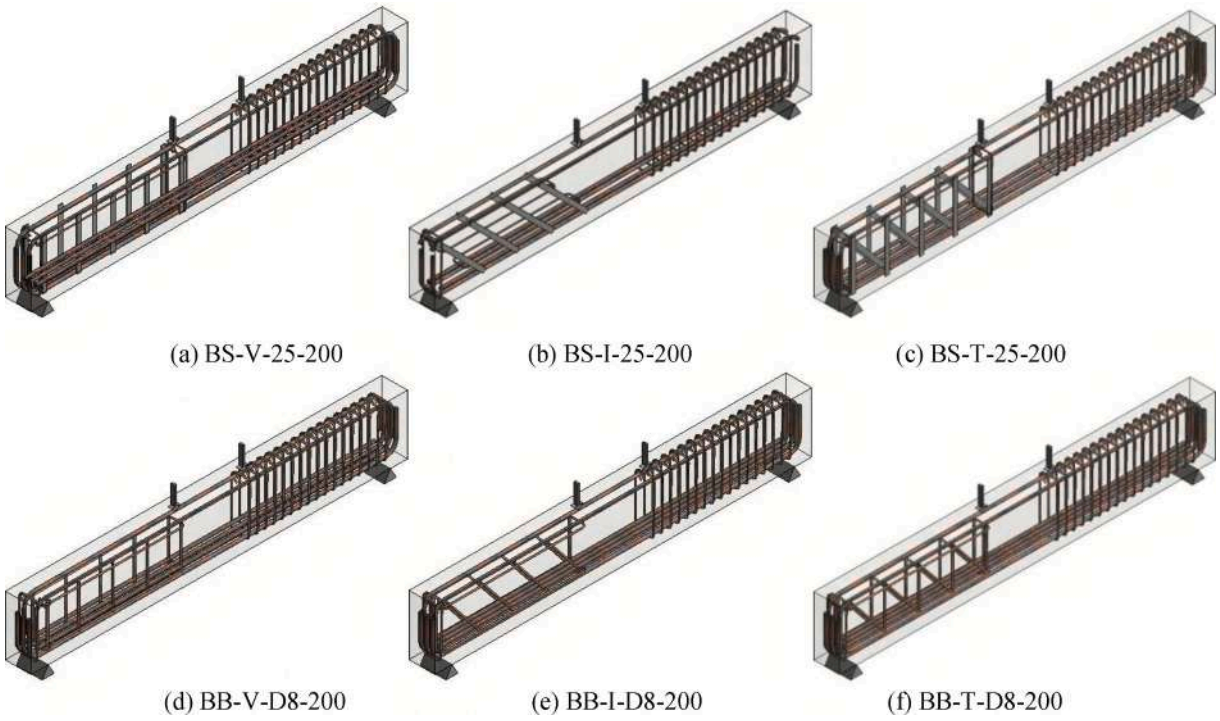


Fig. 2. 3D view showing internal trussed strips in the left shear span zones for all beams of group 2 and their corresponding trussed bars of group 3.

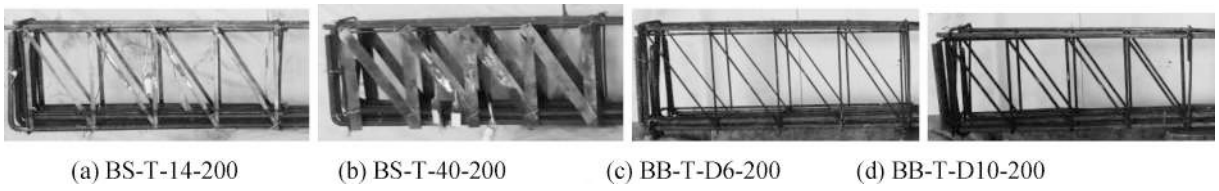


Fig. 3. Images showing internal trussed strips in the left shear span zones for all beams of group 4 and their corresponding trussed bars of group 5.

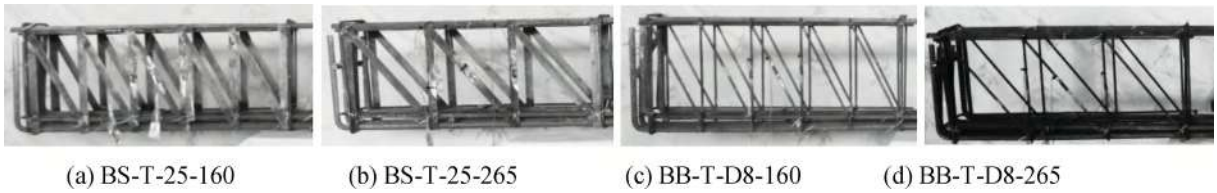
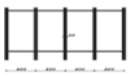
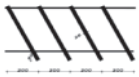
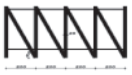
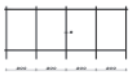
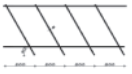
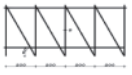
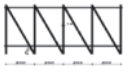
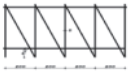
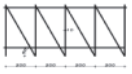
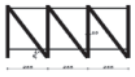
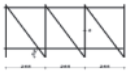


Fig. 4. Images showing internal trussed strips in the left shear span zones for all beams of group 6 and their corresponding trussed bars of group 7.

to the data sheet of the supplier, Portland cement (Type I), crushed limestone having maximum aggregate size of 10 mm and specific gravity of 2.60 was used as coarse aggregate. Besides, the used water/cement ratio (w/c) was about 0.40. In order to estimate the mechanical properties of the used concrete, 15 standard concrete cubes having 150 mm side length and 6 standard cylinders of 150 mm diameter and 300 mm

Table 1
Test matrix.

Group No.	Specimen	Shape of internal reinforcing trusses	Characteristics	Objectives
1	BC	NA	Control un-reinforced beam	Reference beam
2	BS-V-25–200		Vertical strips of 25 mm width and 200 mm spacing	Studying the effect of strips configuration
	BS-I-25–200		Inclined strips of 25 mm width and 200 mm spacing	
	BS-T-25–200		Trussed strips of 25 mm width and 200 mm spacing	
3	BB-V-D8-200		Equivalent vertical bars of 8 mm diameter and 200 mm spacing	Equivalent bar diameter for strip cross-section (25*2) mm and different configuration. Reference for group 2
	BB-I-D8-200		Equivalent inclined bars of 8 mm diameter and 200 mm spacing	
	BB-T-D8-200		Equivalent trussed bars of 8 mm diameter and 200 mm spacing	
4	BS-T-14–200		Trussed strips of 14 mm width and 200 mm spacing	Studying the effect of strips cross-sectional area
	BS-T-40–200		Trussed strips of 40 mm width and 200 mm spacing	
5	BB-T-D6-200		Equivalent trussed bars of 6 mm diameter and 200 mm spacing	Equivalent bar diameter for strip cross-sections used in group (4)
	BB-T-D10-200		Equivalent trussed bars of 10 mm diameter and 200 mm spacing	
6	BS-T-25–160		Trussed strips of 25 mm width and 160 mm spacing	Studying the effect of strip spacing
	BS-T-25–265		Trussed strips of 25 mm width and 265 mm spacing	
7	BB-T-D8-160		Equivalent trussed bars of 8 mm diameter and 160 mm spacing	Equivalent bar spacing used in group (6)
	BB-T-D8-265		Equivalent trussed bars of 8 mm diameter and 265 mm spacing	

NA = not applicable

height were collected and prepared during casting of the beams. And then subjected to the same curing conditions of the test beams where the beams, cubes and cylinders were subjected to wet curing for one week and then left exposed to air drying till the testing day. All beams were tested in two continuous days in order to limit the variation in the shear strength. During testing, the average compressive cube strength based on the results of 15 standard cubes was about 25.4 MPa, while the average indirect tensile strength based on the splitting test on 6 standard cylinders was about 2.85 MPa.

All beams were reinforced with high tensile steel bars of 16 and 18 mm diameters, while the used stirrups were made of smooth mild steel of 8 mm diameter. Besides, the pre-fabricated trussed bars were made of smooth bars having 6, 8 and 10 mm diameters. Furthermore, the pre-fabricated trussed strips were made of mild steel strips having 2 mm thickness. Therefore, in order to determine the mechanical properties for each bar type and size as well as the steel strips, standard tension tests were performed on three typical specimens for each bar type as well as the steel strips. The average mechanical properties for all bar diameters and steel strips are summarized in Table 2.

2.3. Test setup, instrumentation and procedures

All beams were loaded incrementally under four point loading scheme where the shear span-to-depth ratio was kept constant for all beams to be 2.3, in order to ensure the occurrence of shear failure. At the strengthened shear span side, two Linear Variable Differential Transformers (LVDTs) of 100 measuring length were arranged at right angle in order to estimate the developed shear strain on the concrete surface. In addition, one LVDT having 50 mm measuring length was used in order to measure the developed mid-span deflection as shown in Fig. 6. The developed tensile normal strain on the main tensile steel bars was measured using 6 mm gauge length strain gauge mounted at the mid-span region, while two Pi gauges of 100 mm gauge length were used to measure the developed deformations on the concrete surface at both tension and compression sides. Furthermore, the developed normal strains on selected internal members of all trusses near the middle of the shear span were measured by 6 mm gauge length strain gauges. All beams were incrementally loaded up to complete failure where the acting load was measured by a load cell of 600 kN capacity. After each loading step, the vertical mid-span deflection, the readings of the orthogonal LVDTs, the Pi-gauge readings and the developed normal strains in the longitudinal steel bars as well as the internal members of the internal steel trusses were recoded and stored using an automatic data logger unit (TDS-150).

3. Test results and discussion

All beams had been tested up to complete shear failure, while the acting load at different stages was identified and recorded. Besides, the mid-span deflection, the developed tensile strains on both the longitudinal and selected members of the internal steel trusses and the shear crack width at different load level were measured. Table 3 summarizes the experimental results for all beams. In addition, further discussion on the cracking characteristics including cracking load, crack width and crack propagation in addition to the ultimate capacity for all beam are presented and compared herein below.

3.1. Failure modes, cracking and ultimate loads

The control and the reinforced beams by either trussed strips or trussed bars have failed due to compression shear failure as planned. All beams passed by the same cracking scenarios except that the corresponding loads for the key points were differed. The concrete section was uncrack till the concrete tensile resistance was exhausted in flexure then the first flexural crack was developed. Processing with loading, the un-reinforced (control beam) and the reinforced side by internal trusses

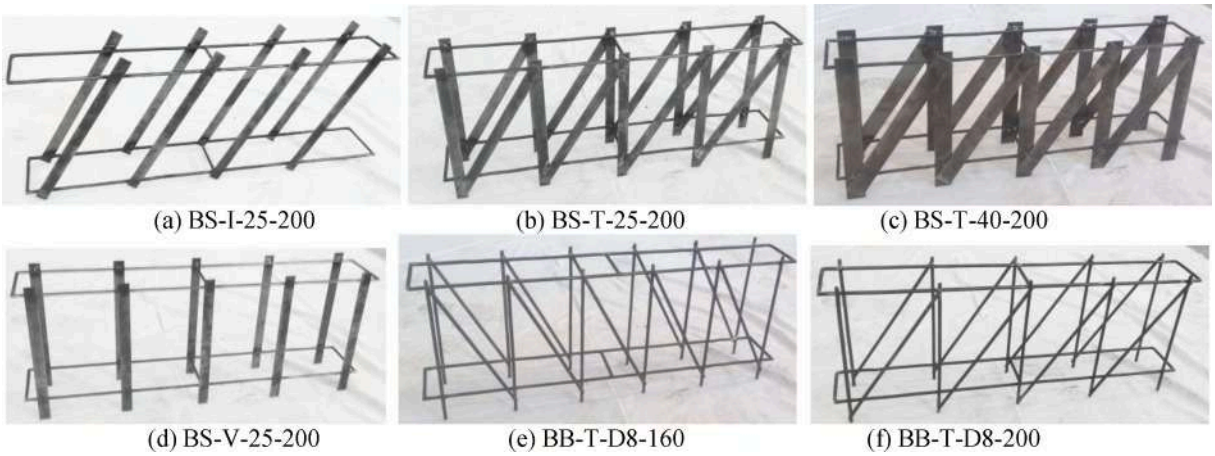


Fig. 5. Selected images showing assembled steel trusses.

Table 2
Mechanical properties of steel bars and steel strips.

Dimensions of steel bar or strip	Type	Average yield stress, MPa	Average tensile strength, MPa	Average modulus of elasticity, GPa
Ø6 bar	Smooth mild steel	358	469	201
Ø8 bar	Smooth mild steel	355	484	201
Ø10 bar	Smooth mild steel	346	458	201
Ø16 bar	Deformed high-tensile	406	624	203
Ø18 bar	Deformed high-tensile	446	637	203
Strip (t = 2 mm)	Smooth mild steel	320	385	202

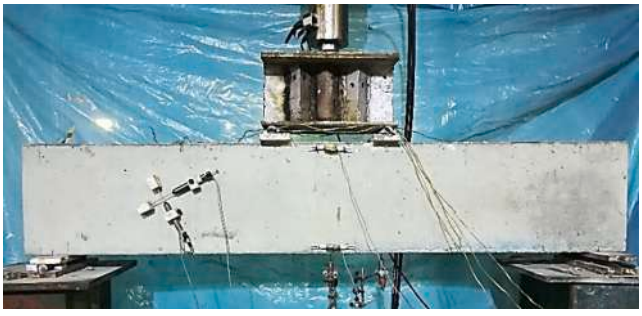


Fig. 6. Test setup and instrumentation.

started to show shear cracking. Soon later, the properly reinforced side with vertical stirrups (right side for all beam) exhibited shear cracking. Finally, proceeding with loading triggered the sudden shear failure for all tested beams. It is worth mentioning that for the reinforced beams with steel trusses, failure occurred after the exhausting the ultimate capacity of the provided steel trusses, which increased the ultimate capacity considerably compared to that of the control beam where the shear resistance for the control beam was provided only by the concrete resistance as well as the dowel action of the longitudinal bars.

The control beam (BC) started to show flexural cracking at a vertical load of about 97 kN. Only beam BB-T-D6-200, which reinforced with trussed bars of 6 mm diameter showed approximately the same cracking load as that developed by control beam. On the other hand, the remaining reinforced beams showed slightly higher flexural cracking loads as listed in Table 3. This means that the used internal steel trusses had insignificant effect on the flexural cracking. However, these internal trusses hindered the appearance of shear cracking at both sides of all reinforced beams.

For the control beam, the un-reinforced side showed first shear crack at a vertical load of about 151 kN. By using vertical (BS-V-25–200), inclined (BS-I-25-200) and trussed strips (BS-T-25-200), the corresponding shear cracking loads were increased by about 16%, 40% and 47% compared to that of the control beam (BC). Using equivalent trusses based on equivalent bar diameter of 8 mm resulted in reducing the increases to be 13%, 25% and 34%, for beams BB-V-D8-200, BB-I-D8-200 and BB-T-D8-200, respectively. This means that using steel strips is better than rounded steel bars in delaying the appearance of the shear cracking by about 3%, 15% and 13%, respectively, for vertical, inclined and trussed configurations.

Reducing the width of the trussed strip from 25 mm to 14 mm resulted in reducing cracking shear enhancement from 47% to 23%. As for the equivalent bar diameter of 6 mm (BB-T-D6-200), the cracking shear enhancement reduced to be 13%. On contrary, increasing the size of steel strip to be 40 mm (BS-T-40-200) and the equivalent bar diameter to be 10 mm (BB-T-D10-200) resulted in cracking shear enhancement of about 49% and 37%, respectively. In sum, using steel strips to form the truss members is better than using equivalent rounded steel bars since the steel strips hindered the appearance of the shear cracks significantly compared to those corresponding to rounded steel bars. This enhancement is directly proportional to the size of both steel strips and bars.

Varying the spacing between the vertical members for the trussed strips to be 160 mm (BS-T-25-160) or 265 mm (BS-T-25-265) resulted in changing the shear cracking enhancement to 49% and 34%, respectively. This means that the effect of strip size has a small effect on the shear cracking enhancement for trussed strips. On contrary, the effect of bar size has insignificant effect on the shear cracking enhancement for trussed bars based on the results of beams BB-T-D8-160 and BB-T-D8-265, where the shear cracking loads were 208 and 202 kN, respectively.

As for the ultimate capacity, the trussed configuration showed the highest increase in the ultimate capacity since the increases in the ultimate capacities were about 68, 94 and 126% for beams BS-V-25-200, BS-I-25-200 and BS-T-25-200, respectively. Besides, the trusses made of steel strips showed higher increases in the ultimate capacity compared to those made of equivalent steel bars. Table 3 showed the percentage of increases in the ultimate capacity for all beams compared to that of the control beam (BC). The increases in the ultimate capacity for beams BS-V-25-200, BS-I-25-200 and BS-T-25-200 were about 10%, 17% and 10% compared to those for beams BB-V-D8-200, BB-I-D8-200 and BB-T-D8-200, respectively.

As the cross-sectional dimensions changes, the increases in the

Table 3
Experimental results.

GroupNo.	Specimen	$P_{cr,f}$(kN)	$P_{cr,sh}$ (kN) Left side*	Right side**	P_u (kN)	$\Delta_{maximum}$(mm)	Developed tensile strain on longitudinal steel bars at failure, micro-strain	Increase in P_u compared to BC (%)
1	BC	97	151	161	189.0	4.2	726	–
2	BS-V-25-200	103	175	203	317.6	7.3	1726	68.04
	BS-I-25-200	103	212	212	366.2	8.2	1808	93.76
	BS-T-25-200	104	222	227	426.7	7.5	2210	125.77
3	BB-V-D8-200	101	170	190	287.7	5.6	829	52.22
	BB-I-D8-200	102	188	200	314.2	5.9	1554	66.24
	BB-T-D8-200	101	203	209	370.7	7.2	1987	96.14
4	BS-T-14-200	108	185	194	289.3	6.2	1415	53.07
	BS-T-40-200	106	225	227	437.0	6.7	2043	131.22
5	BB-T-D6-200	97	170	188	240.4	5.2	792	27.20
	BB-T-D10-200	103	207	215	373.3	5.6	992	97.51
6	BS-T-25-160	105	225	217	454.9	6.9	1521	140.69
	BS-T-25-265	104	203	207	364.0	6.3	1335	92.59
7	BB-T-D8-160	103	208	210	386.2	6.6	1967	104.34
	BB-T-D8-265	100	202	200	336.6	6.6	1575	78.10

$P_{cr,f}$ = First flexural cracking load, $P_{cr,sh}$ = First shear cracking load, P_u = Failure load, * left side reinforced with trussed steel assembly. ** right side reinforced with closely spaced vertical stirrups, $\Delta_{maximum}$ = maximum mid-span deflection corresponding to maximum load.

ultimate capacity for beams BS-T-14-200 and BS-T-40-200 were about 20% and 17% compared to those for beams BB-T-D6-200 and BB-T-D10-200, respectively. As for the spacing effect, the increases in the ultimate capacity for beams BS-T-25-160 and BS-T-25-265 were about 18% and 8% compared to those for beams BB-T-D8-160 and BB-T-D8-265, respectively. In average sense, the ultimate capacity for reinforced concrete beam provided with internal truss made of steel strips is higher than the corresponding capacity of beam reinforced by equivalent rounded trussed bars by about 16%.

For the control beam (BC), the developed normal strain on the main tensile steel at failure was about 726 micro-strain, which corresponding to about 0.33 times the yielding strain of the used bars (2197 micro-strain). Providing internal steel trusses formed from either steel strips or rounded steel bars resulted in increased flexural capacity. However, the developed normal strain on the longitudinal bars did not reach the yielding strain for all beams except that for beam BS-T-25-200 whose developed strain exceeded slightly the yielding strain as listed in Table 3.

Fig. 7 shows the developed shear failure of the control beam (BC) just before the occurrence of the sudden shear failure. It can be noticed that the shear cracking initiated at the mid-height of the cross-section and then propagated in the line direction connecting the acting load and reaction force. Fig. 8 shows the developed shear failure of all beams for both groups 2 and 3 just before the occurrence of the sudden shear failure. It can be observed that the cracking and failure pattern for all beams reinforced with trusses strips showed approximately the same cracking and failure pattern as those exhibited by the corresponding beams reinforced with equivalent trussed bars. The same observation was noticed when varying the cross-sectional dimensions of the truss members as depicted in Fig. 9. However, the failure of beam BB-T-D10-200 was more stringent than that exhibited by the corresponding trussed beam BS-T-40-200 (refer to Fig. 9(b and d)). This means that the trussed strips confined the concrete at the core section more effectively than the trussed bars, which led to increase the shear capacity of beam BS-T-40-200 significantly compared to that of beam BB-T-D10-200 showing alleviated shear failure compared to that developed by beam BB-T-D10-200.

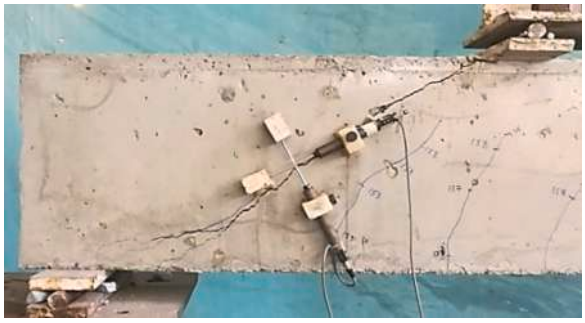


Fig. 7. Shear failure of control beam BC.

Decreasing the spacing between the vertical members resulted in increased the shear capacity significantly as developed by beam BS-T-25-160. Therefore, the exhibited shear failure was more severe and explosive than that showed by the corresponding beam BB-T-D8-160 based on trussed bars where the sustained load by beam BB-T-D8-160 was lower than that carried by beam BS-T-25-160 by about 15%, refer to Fig. 10(a) and 10(c). At lower loading level, when the shear capacity was decreased as a result of increased spacing, the cracking pattern for both beams BS-T-25-265 and BB-T-D8-265 was approximately the same as depicted in Fig. 10(b) and 10(d).

In order to get insight on the internal cracks after complete failure for all beams, the concrete cover was revealed at the strengthened side and then the inclination angle of the major shear crack was measured and the location between the major shear crack and the middle of the shear span was also measured at the mid-height of the beam's cross-section as summarized in Table 4. It is recognizable that the inclined member of the truss has to be perpendicular to the developed shear cracks in order to obtain the most significant performance. Therefore the complementary angles for the inclined members were also estimated. In addition, the differences between the actual inclination angle of the developed major shear crack and the complementary angles were calculated as presented in Table 4.

For the trusses made of vertical members only, the inclination angles of the developed major shear cracks for beams BS-V-25-200 and BB-V-D8-200 were 44° and 45°, respectively. While, the center of the developed major shear crack for BS-V-25-200 was closer than to the center of the shear span zone compared to that of BB-V-D8-200 as depicted in Fig. 11(a) and 11(b). That could enable the trussed strips to resist shear

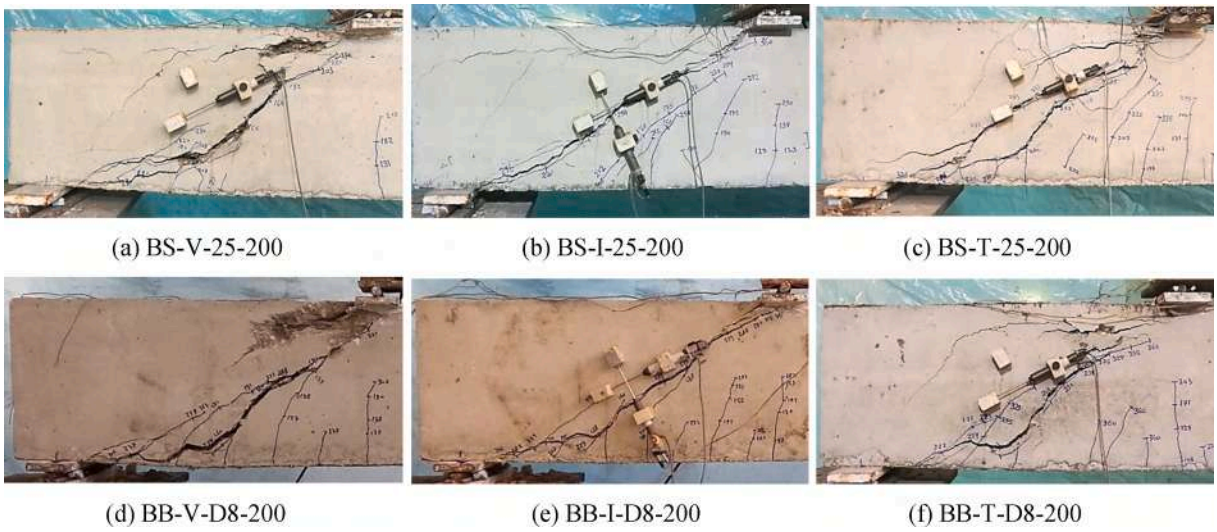


Fig. 8. Shear failure of all beams of groups 2 and 3.

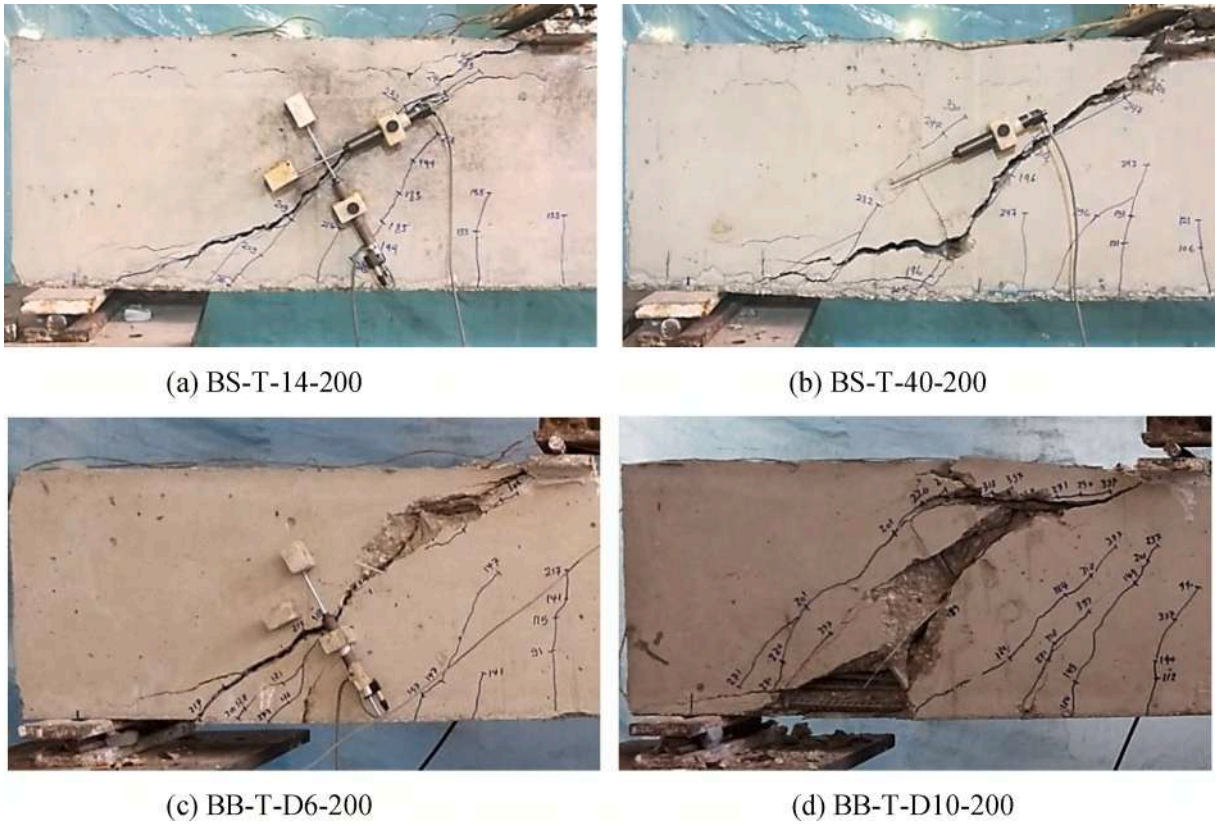


Fig. 9. Shear failure of all beams of groups 4 and 5.

stress more than trussed bars. As for inclined and trussed configuration, the same observation was observed since the developed major shear cracks of beams BS-I-25-200 and BS-T-25-200 were closer than to the center of the shear span zone compared to those of beams BB-I-D8-200 and BB-T-D8-200 as depicted in Fig. 11(c) to 11(f). The most important observation was that the developed shear cracks of trussed strips were more close to the complementary angles for the inclined members. This means that the developed shear cracks were close to be perpendicular to the inclined members for the trusses made of steel strips. That can explain the reason for higher shear resistances of trussed strips than that developed by trussed bars.

The above conclusion could be generalized for different cross-sectional dimensions of the truss members as well as when the spacing between vertical member was varied as illustrated in Figs. 12 and 13. It is worth mentioning that the internal trusses made of either steel strips or rounded steel bars were fully integrated after the complete failure that assures the quality of the used welding to assemble the trusses. However, some images in Figs. 11 to 13, showed broken members especially for trussed strips. That was happened during removing concrete cover process.

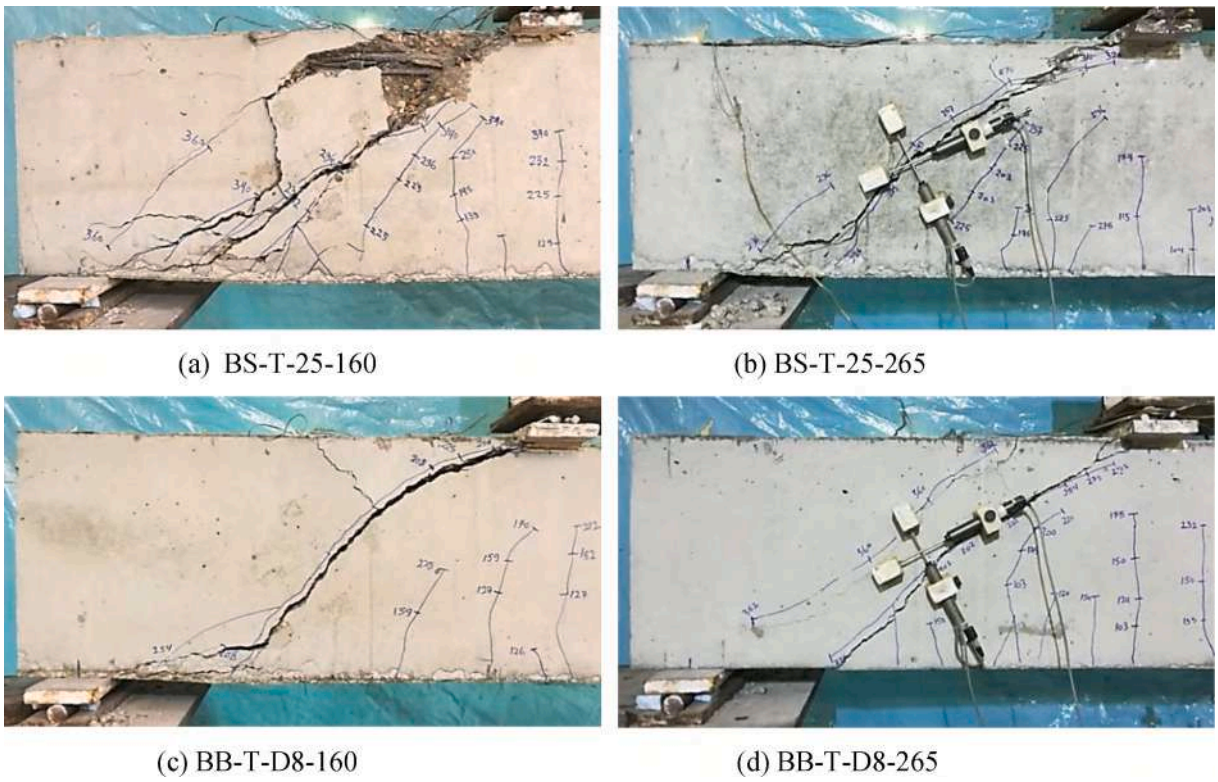


Fig. 10. Shear failure of all beams of groups 6 and 7.

Table 4
Major shear crack characteristics.

Group No.	Specimen	Components of internal truss	θ_I	θ_C	θ_M	$\theta_M - \theta_C$	X, mm
1	BC	NA	—	——	—	——	–
2	BS-V-25-200	Strips	90°	NA	44°	NA	136
	BS-I-25-200	Strips	60°	30°	38°	8°	12
	BS-T-25-200	Strips	60°	30°	37°	7°	0
3	BB-V-D8-200	Bars	90°	NA	45°	NA	160
	BB-I-D8-200	Bars	60°	30°	39°	9°	130
	BB-T-D8-200	Bars	60°	30°	44°	14°	92
4	BS-T-14-200	Strips	60°	30°	39°	9°	51
	BS-T-40-200	Strips	60°	30°	48°	18°	97
5	BB-T-D6-200	Bars	60°	30°	45°	15°	75
	BB-T-D10-200	Bars	60°	30°	50°	20°	54
6	BS-T-25-160	Strips	65°	25°	34°	9°	70
	BS-T-25-265	Strips	53°	37°	40°	3°	13
7	BB-T-D8-160	Bars	65°	25°	49°	24°	33
	BB-T-D8-265	Bars	53°	37°	32°	−5°	33

NA = not applicable, θ_I = inclination angle of truss members, θ_C = complementary angle to the inclination angle of truss members, θ_M = measured shear crack angle, X = distance between center of the major shear crack and center of shear span zone

3.2. Load-deflection response

Fig. 14 shows relationships between the total acting load and the mid-span deflection for all beams of groups 2 and 3 as well as the control beam (BC). For all beams, it can be observed that the relationship was approximately linear up to near the ultimate load; however, some nonlinearity was exhibited just before the sudden shear failure owing to the concrete cracking. In addition, the control beam (BC) showed the lowest flexural stiffness at any load level among all beams.

For the beams reinforced with vertical or inclined members only, the load-deflection curves for both configurations based on either strips or rounded bars were approximately similar till the failure of beams reinforced with bars assemblies at lower loads compared to those reinforced with strips assemblies. On the other hand, using trussed strips as beam BS-T-25-200 resulted in improving the flexural stiffness from the beginning of loading till complete failure compared to the corresponding beam reinforced with trussed bars (BB-T-D8-200). Varying the cross-sectional dimensions of the truss members assured the former observations where the developed deflection by the beam reinforced with trussed strips was smaller than the corresponding deflection developed by the opponent beam reinforced with equivalent trussed bars as depicted in Fig. 15 for BS-T-14-200 versus BB-T-D6-200 and BS-T-40-200 versus BB-T-D10-200. Changing the spacing between the vertical members of the internal trusses led to the same conclusion where the flexural stiffness of the beam reinforced with trussed strips is higher than the correspond one for the beam reinforced with equivalent trussed bars as depicted in Fig. 16 (compare BS-T-25-160 and BB-T-D8-160, BS-T-25-265 and BB-T-D8-265).

3.3. Developed normal strain on the internal members of steel trusses

For all reinforced beams using internal steel trusses based on either steel strips or steel rounded bars, the developed normal strains on selected members near the middle of the shear span zone during loading till complete failure were measured. Based on the obtained mechanical

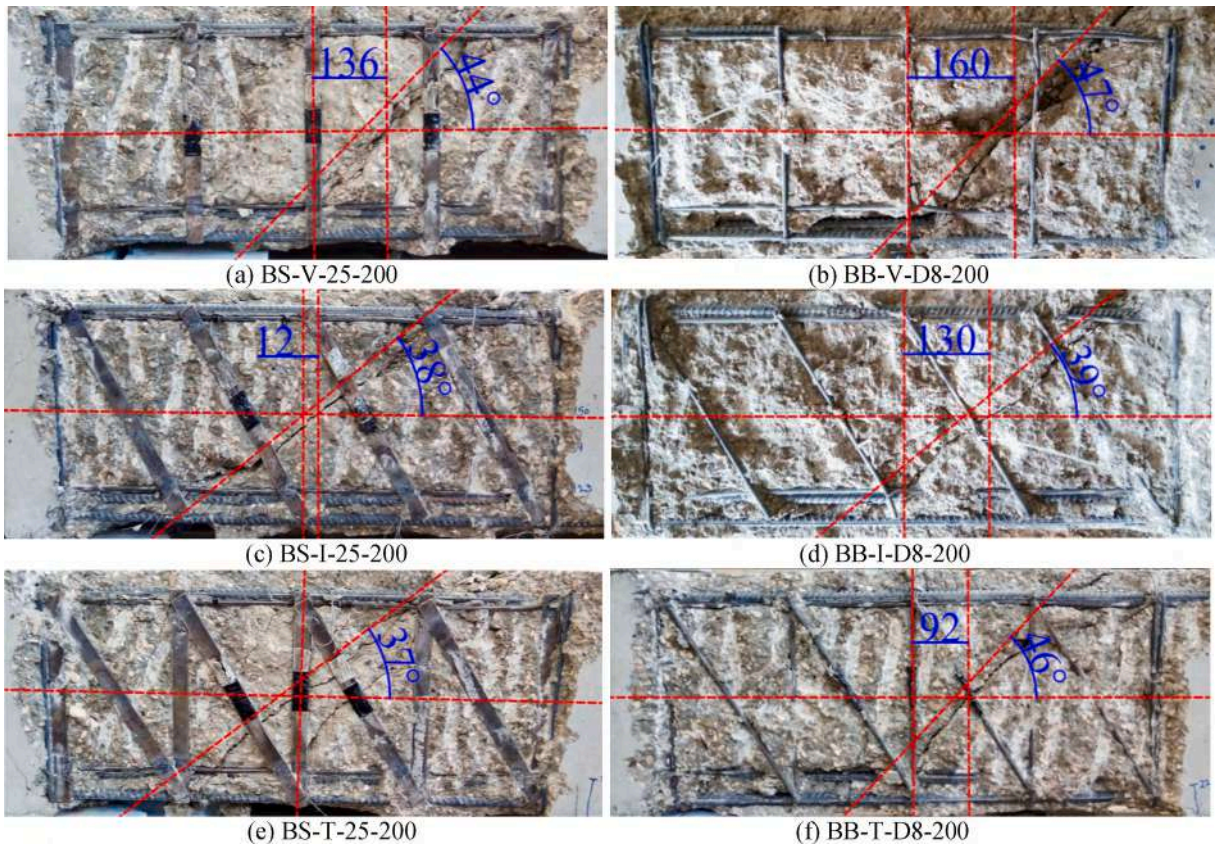


Fig. 11. Developed shear failure inside the concrete core after taking out the side concrete cover for all beams of groups 2 and 3.

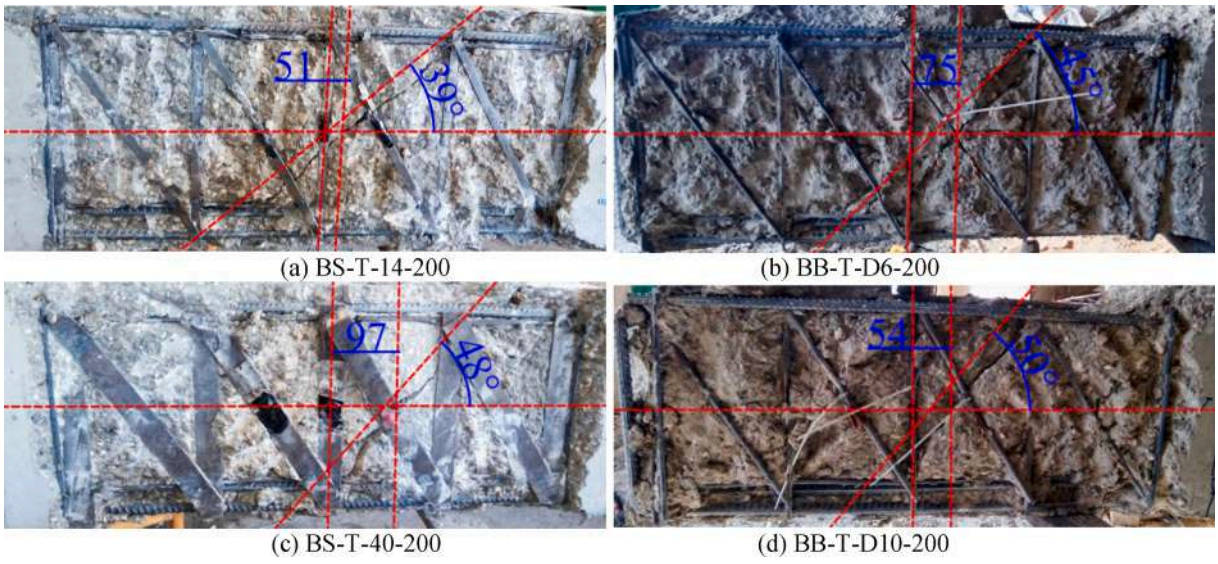


Fig. 12. Developed shear failure inside the concrete core after taking out the side concrete cover for all beams of groups 4 and 5.

properties of the used steel strips and the rounded steel bars having 6, 8 and 10 mm diameter as given in Table 2, the yielding strains were about 1584, 1781, 1766 and 1721 micro-strain, respectively. Besides, after complete failure of all strengthened beams, the concrete cover at the failed shear span zone was removed in order to expose the steel truss as well as the major shear crack as depicted in Figs. 11 to 13.

Fig. 17(a) and 17(b) show the developed normal strains, up to failure, on the internal members of steel trusses formed from vertical steel strips and vertical rounded steel bars, respectively. It can be noticed that only the strain on location (2) exceeded the yielding point for both beams having steel strips and bars. With the aid of the location of the developed major shear cracks depicted in Fig. 11(a) and 11(b), it can be noticed that the developed major shear cracks for beams BS-V-25-200 and BB-V-D8-200 laid between members having numbers (2) and (3) but more close to location (2). Thus, the members at location (2) stressed more than the other member till they exceeded the yield points. On the other hand, the developed strains on location (4) for both beams exhibited very small value because they located away from the

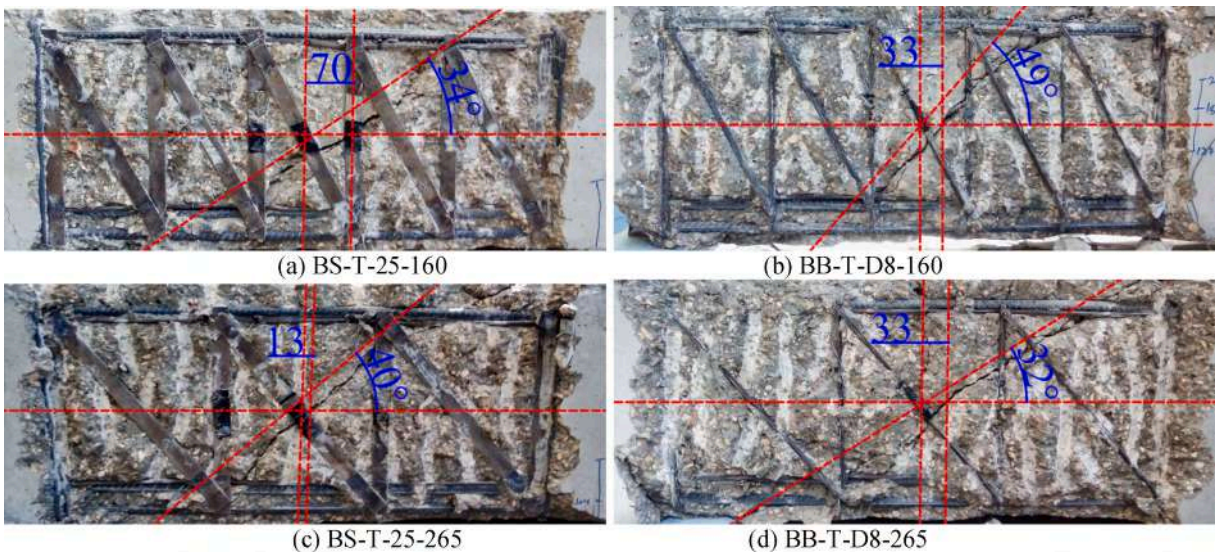


Fig. 13. Developed shear failure inside the concrete core after taking out the side concrete cover for all beams of groups 6 and 7.

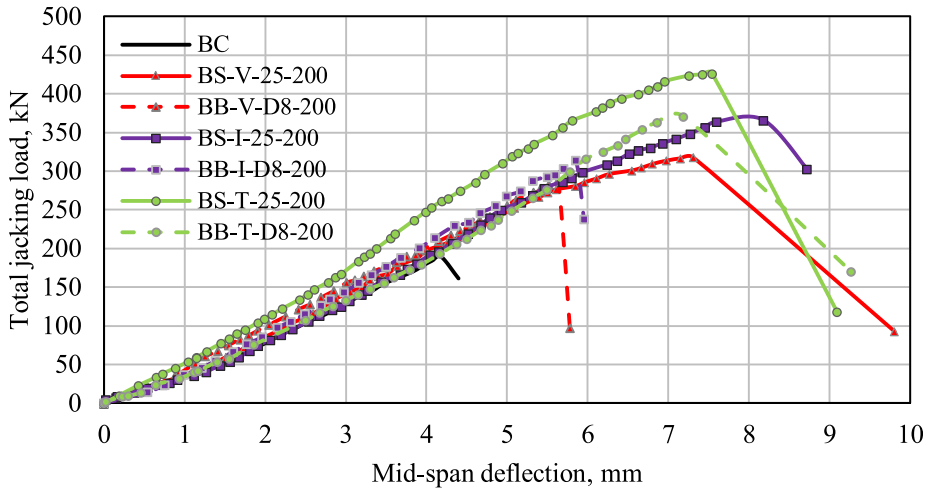


Fig. 14. Total load versus mid-span deflection relationships for all beams of groups 2 and 3.

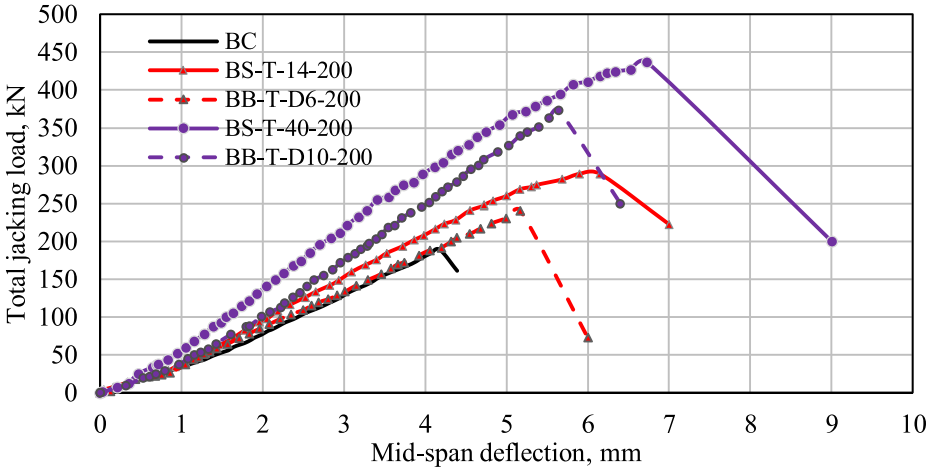


Fig. 15. Total load versus mid-span deflection relationships for all beams of groups 4 and 5.

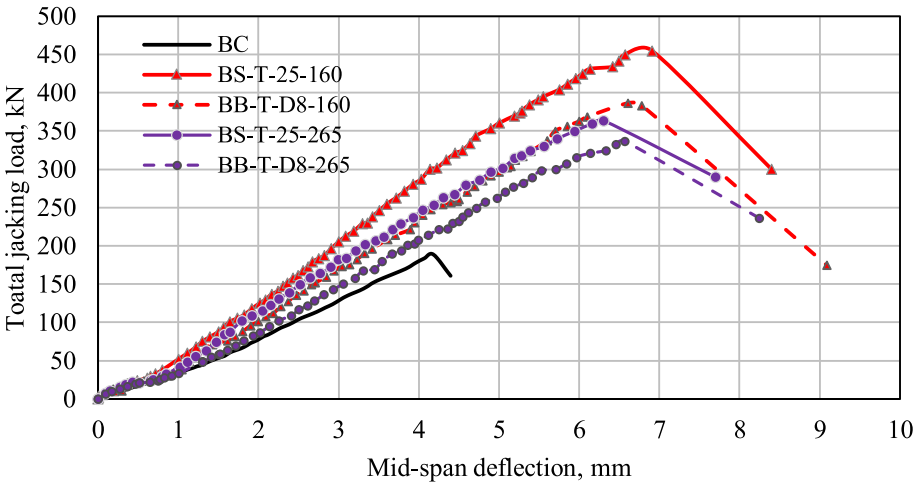


Fig. 16. Total load versus mid-span deflection relationships for all beams of groups 6 and 7.

developed major shear cracks.

For inclined configuration of steel strips, it was noticed that the developed normal strains at locations (2) and (3) exceeded the yield point for beam BS-I-25-200 as shown in Fig; 17(c). That is because the developed major shear crack for this beam passed between locations (2) and (3) but was closer than to location (2) as depicted in Fig. 11(c). On contrary, only the developed strain at location (2) for beam BB-I-D8-200 yielded as depicted in Fig. 17(d). That is because the developed major shear crack for this beam passed by the center of the bar having location (2) as depicted in Fig. 11(d).

As for truss configuration of steel strips (BS-T-25-200), it was noticed that the developed normal strain at locations (2) and (4) exceeded the yield point as depicted in Fig. 17(e). That is because two major shear cracks were developed; one of them passed by the center of the member having location (2) and the other one intersected the member having location (4) near its mid-height as depicted in Fig. 11(e). Unfortunately, the strain at location (3) for this beam has been damaged during the test. As for the corresponding beam reinforced with equivalent trussed bars (BB-T-D8-200), the developed major shear crack passed by the center of the inclined member having location (2) as depicted in Fig. 11(f). This explains the reason for yielded the strain at location (2) only for beam BB-T-D8-200 as depicted in Fig. 17(f). Also, the strain at location (3) for this beam has been damaged during the test.

Fig. 18 shows the developed normal strains on the selected members of internal trusses for all beams of groups 4 and 5 having different cross-sectional dimensions of the truss member formed from either steel strips or rounded steel bars. Similarly, the results of the developed strains on the selected locations can be explained with the aid of Fig. 12 showing the locations of the developed major shear cracks. Unfortunately, the strains at some locations were defected after casting the beams such as location (2) for beam BB-T-D6-200 and location (3) for beam BS-T-40-200.

Fig. 19 shows the developed normal strains on selected members of internal trusses for all beams of groups 6 and 7 having different spacing between vertical members of the trusses formed from either steel strips or rounded steel bars. Also, the results of the developed strains on the selected locations can be explained with the aid of Fig. 13 showing the locations of the developed major shear cracks. Unfortunately, the strains at some locations were defected after casting the beams such as location (4) for beam BS-T-25-160, location (4) for beam BB-T-D8-160, location (4) for beam BS-T-25-265 and, location (4) for beam BB-T-D8-265.

3.4. Comparisons between the experimental shear capacities and the analytical estimations

In order to validate the accuracy of the obtained experimental results, the model proposed by [52] was selectively chosen to obtain the analytical shear resistances of the tested beams. The adopted model was used to calculate the analytical shear resistance of strengthened reinforced concrete beams using composite plates taking into account the contribution of vertical stirrups and neglecting the concrete tensile resistance. Thus, the ultimate shear capacity of reinforced concrete beams with internal steel trusses, V_{st}, can be calculated by Eq. (1) [52].

$$V_{st} = \frac{A_v f_v d_v}{s.tan\theta} + \frac{A_m f_m d_m}{s_m}\left(\frac{1}{tan\theta} + \frac{1}{tan\alpha}\right) sin\alpha \quad (1)$$

Where A_v = the cross-sectional area of either vertical steel strips or steel bars; f_v = the yielding stress of the used strips/bars as given in Table 2 divided by strength reduction factor of 1.15; d_v = effective depth of the beam' cross-section; s = spacing between the vertical members; θ = inclination angle of the major shear crack width as given in Table 4. A_m = the cross-sectional area of either inclined steel strips or steel bars; f_m = the yielding stress of the used strips/bars as given in Table 2 divided by strength reduction factor of 1.15; d_m = vertical projection of the steel strip/ plate; s_m = horizontal spacing between the inclined members; α = inclination angle of the inclined member with horizontal. For calculating the shear capacity of the control beam (BC), the shear capacity was calculated for un-cracked section by multiplying the concrete shear strength per ECP 203-2019 [31] as given in Eq. (2) by the effective cross-sectional area (width × effective depth). Besides, the considered experimental shear resistance for the control beam was that corresponding to the cracking shear force at the unreinforced side as given in Table 3.

$$q_{c(uncrcaked)} = 0.16\sqrt{\frac{f_{cu}}{\gamma_c}} \quad (2)$$

The total analytical shear resistance was the summation of the shear resistance of the steel truss and the contribution of cracked concrete by multiplying the concrete shear strength per ECP 203-2019 [31] as given in Eq. (3) by the effective cross-sectional area (width × effective depth).

$$q_{c(crcaked)} = 0.12\sqrt{\frac{f_{cu}}{\gamma_c}} \quad (3)$$

Table 5 summarizes the results of both experimental test and the analytical model. It can be observed that the analytical model showed conservative results and sufficient safety margins for all tested beams

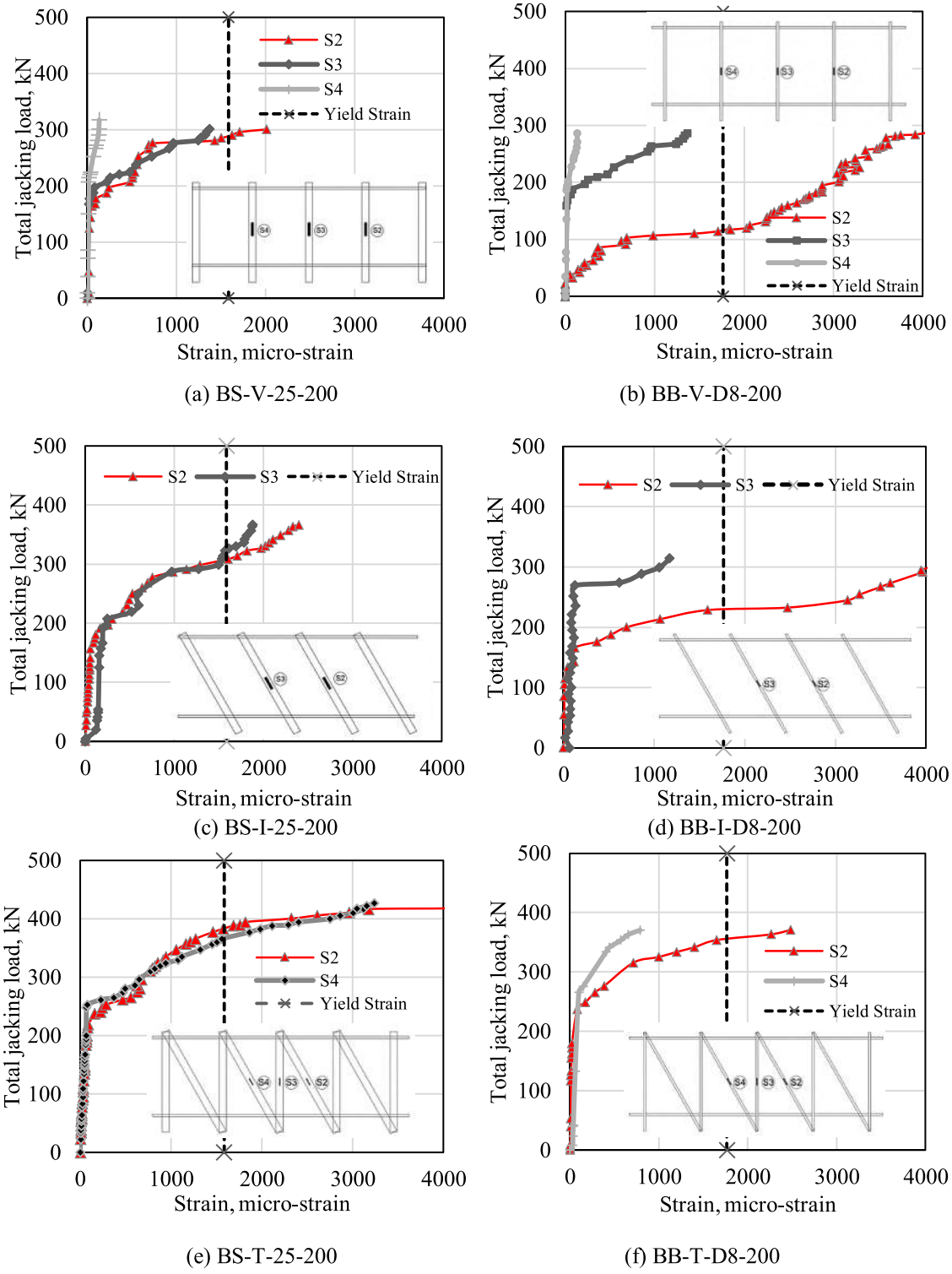


Fig. 17. Developed normal strains on selected members of internal trusses for all beams of groups 2.

when the contribution of the cracked concrete strength was neglected. On contrary, when the contribution of the cracked concrete was considered, three beams; namely, BB-T-D10-200, BS-T-25-160 and BB-T-D8-265 showed over estimation of the analytical capacity by about 9%, 2% and 5%, respectively. As for, beam BB-T-D10-200, the experimental capacity was somewhat lower than the expected capacity compared to the capacity of beam BB-T-D8-200 where beam BB-T-D8-200 sustained failure total load of about 370.7 kN, while beam BB-T-D10-200 sustained about 373.3 kN, which is relatively small enhancement compared to the increased cross-sectional area of the used steel bar. In addition, the exhibited failure of beam BB-T-D10-200 as depicted in Fig. 9(d) was more stringent than that exhibited by BB-T-D8-200 as depicted in Fig. 8 (f), especially the ultimate loads are close to each other. Maybe some error occurred during testing of beam BB-T-D10-200.

As for beams BS-T-25-160 and BB-T-D8-265, the slight over estimation came from that the used inclination angles in Eq. (1) were 34° and 32°, respectively, as obtain from the experimental testing. If the used angles were 45°, the safety margins could be 29% and 27% respectively.

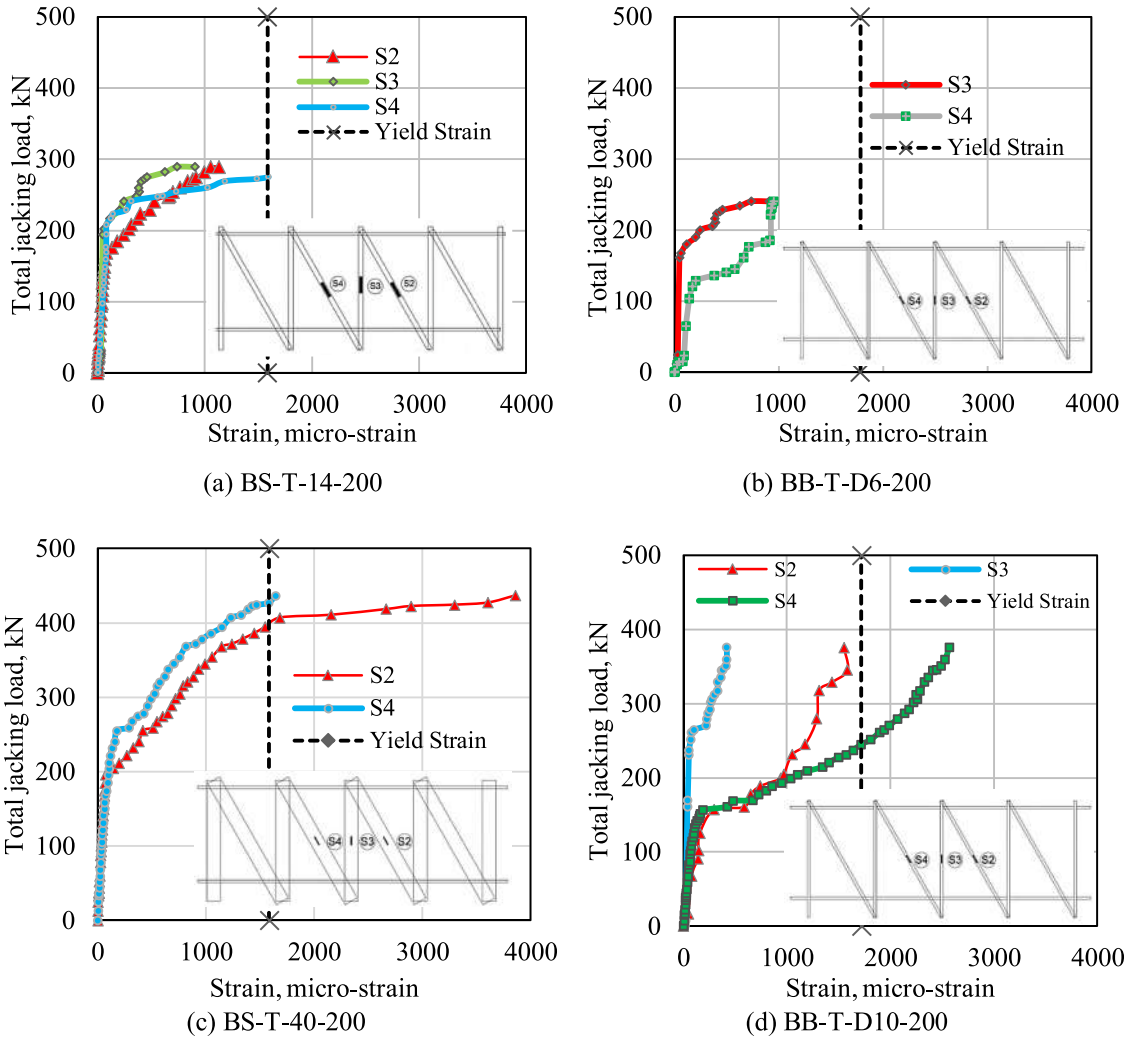


Fig. 18. Developed normal strains on selected members of internal trusses for all beams of groups 4 and 5.

In general, the experimental results showed comparable results with the analytical calculations based on the resulted of the adopted model. Neglecting the contribution of the cracked concrete showed the adequacy of the used internal steel trusses in resisting the acting shearing load.

3.5. *Developed major shear crack width versus the applied loading*

In the current paper, the effect of providing internal steel trusses made of either steel strips or rounded steel bars on the major shear crack width was investigated taking into account the effect of configuration of the members, cross-sectional area of the truss members and the spacing between the vertical members. For all beams, during testing, the developed major shear crack widths were measured at different load levels using optical microscope of 0.01 mm accuracy. For safety precautions, measuring of shear crack width was stopped near failure.

Fig. 20 shows the growth of the major shear crack width with loading up to near the collapse load for all beams of groups 2 and 3. It can be observed that the control beam BC exhibited the lowest shear cracking load among all beams. In addition, the major shear crack width was increased swiftly after the initiation of cracking. Increasing the applied load resulted in increase the shear crack width, while the configurations of the truss members affected significantly on the developed shear crack width. At the same loading level, beam BB-V-D8-200 reinforced with vertical bars showed the widest shear crack width, while beam BS-T-25-200 reinforced with trussed strips exhibited the narrowest shear crack width. For inclined members' configuration, the shear crack width showed intermediate value between the vertical and trussed configurations for both steel strips and bars.

The most important observation was that the developed shear crack width at any load level for beam reinforced with trussed strips was narrower than the developed shear crack width for the corresponding beam reinforced with equivalent trussed rounded bars. This can be attributed to the increased surface area of the steel strips intersecting with the shear cracks, which restrains the growth of the crack width effectively in comparison with rounded steel bar. Besides, the greater surface area of the trussed strips maintained the confinement of the concrete core of inside the section leading to enhanced shear resistance and accordingly decreases the exhibited shear crack width compared to the case of trussed bars.

Decreasing the cross-sectional area of the truss member made of either steel strips or steel bars resulted in increase the major shear crack width in faster rate compared to the former dimensions and vice versa as depicted in Fig. 21. However, the same conclusion still valid that the developed shear crack width at any load level for beam reinforced with trussed steel strips was narrower than the developed shear crack for the corresponding beam reinforced with equivalent trussed bars. For beam BB-T-D6-200 formed from rounded bars of 6 mm diameter, the last measured cracks width was about 0.25 mm corresponding to a total load of about 239 kN, while the corresponding crack widths for beams BB-T-D8-200 and BB-T-D10-200 at the same load level (239 kN) were about 0.12 mm and 0.10 mm, respectively. As for trussed strips, beam BS-T-14-

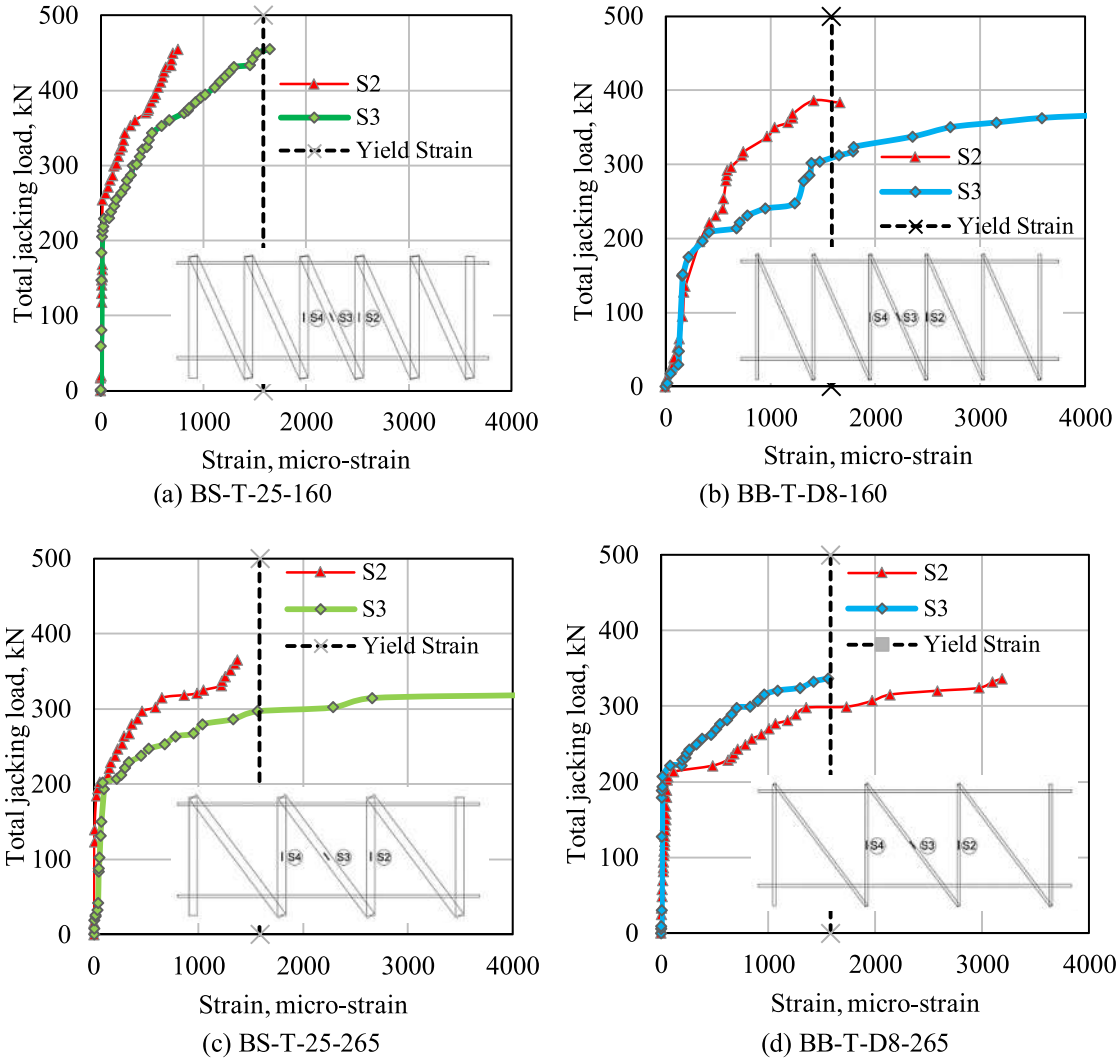


Fig. 19. Developed normal strains on selected members of internal trusses for all beams of groups 6 and 7.

200 showed major crack with of about 0.62 mm corresponding to a total load of about 289 kN. While, beams BS-T-25-200 and BS-T-40-200 exhibited major crack widths of about 0.11 mm and 0.09 mm, respectively, at the same load level of about 289 kN.

For both trussed strips and bars, increasing the spacing between the vertical members resulted in increased the major shear crack width at the same loading level and vice versa as depicted in Fig. 22. Similarly, the developed shear crack width at any load level for beam reinforced with trussed steel strips was narrower than the developed shear crack for the corresponding beam reinforced with equivalent trussed bars.

3.6. Estimation of maximum shear crack width

Researchers showed that the maximum shear crack width is mainly dependent on different parameters such as the developed normal strain on the longitudinal tensile steel, the amount and distribution of the transverse web reinforcement and the side concrete cover at the shear span zone [53,54]. However, few years later, it was found that the effect of side concrete cover in reinforced concrete beams was not well pronounced [55]. Other influencing factors on the shear crack width were also studies such as bond characteristics of the web reinforcement, spacing, angle with member axis and shear span-to-depth ratio [56–59]. In addition, others highlighted the major effect of the stirrups ratio [60,61], the concrete compressive strength [62], and the size effect [63,64]. Furthermore, others showed that the developed strain in the web reinforcement is the most significant parameter affecting shear crack width in reinforced concrete beams [55,58,60]. It is worth mentioning that the available design guidelines for controlling the cracking of reinforced concrete members including crack width and spacing are mostly pertaining to flexural cracking whereas there is a little mention on shear crack width in reinforced concrete members [65]. However, great effort had been done in order to identify the controlling parameters on the shear crack width, and then proposed empirical equations to calculate the shear crack width. Herein below selected empirical expressions have been presented and then used to calculate the shear crack width of the current study in order to verify the applicability and adequacy of such expressions.

Hassan et al. [58] proposed Eq. (4) for estimating the average shear crack width (w_{av}).

$$w_{av} = \left(\frac{\varnothing}{1000}\right) S \frac{k_1 k_2}{\left(\frac{\rho_w}{0.004}\right)^{1.3} \left(\frac{f_c'}{19.6}\right)^{2/3}} \tag{4}$$

Where $\varnothing$ is the shear reinforcement diameter; S is the normalized slip of the shear reinforcement $= 4\text{x}10^3\varepsilon_w + 2\text{x}10^6(\varepsilon_w)^2$ for smooth bars; ε_w is the shear reinforcement strain; $k_1 = 2.4$ for smooth bars; k_2=1.2 for vertical stirrups and 1.0 for inclined stirrups;ρ_w is the shear reinforcement ratio; f_c' is the concrete cylinder compressive strength.

Table 5
Comparisons between calculated ultimate shear load and test results of all beams.

Group No.	Specimen	Test results Q_{Exp}, kN	Analytical results Q_{Ana} (1), kN	Q_{Exp} / Q_{Ana} (1)	Analytical results Q_{Ana} (2), kN	Q_{Exp} / Q_{Ana} (2)
1	BC	75.50	46.09	1.64	—	—
2	BS-V-25-200	158.80	85.00	1.87	50.43	3.15
	BS-I-25-200	183.10	112.90	1.62	78.33	2.34
	BS-T-25-200	213.35	179.50	1.19	144.93	1.47
3	BB-V-D8-200	143.85	88.92	1.62	54.35	2.65
	BB-I-D8-200	157.10	119.86	1.31	85.29	1.84
	BB-T-D8-200	185.35	166.76	1.11	132.19	1.40
4	BS-T-14-200	144.65	111.04	1.30	76.47	1.89
	BS-T-40-200	218.50	204.43	1.07	169.86	1.29
5	BB-T-D6-200	120.20	107.53	1.12	72.96	1.65
	BB-T-D10-200	186.65	205.34	0.91	170.77	1.09
6	BS-T-25-160	227.45	232.33	0.98	197.76	1.15
	BS-T-25-265	182.00	135.47	1.34	100.90	1.80
7	BB-T-D8-160	193.10	175.85	1.10	141.28	1.37
	BB-T-D8-265	168.30	177.31	0.95	142.74	1.18

Q_{Ana} (1) = analytical shear resistance taking into account the contribution of cracked concrete, Q_{Ana} (2) = analytical shear resistance for the internal steel truss only neglecting the effect of cracked concrete

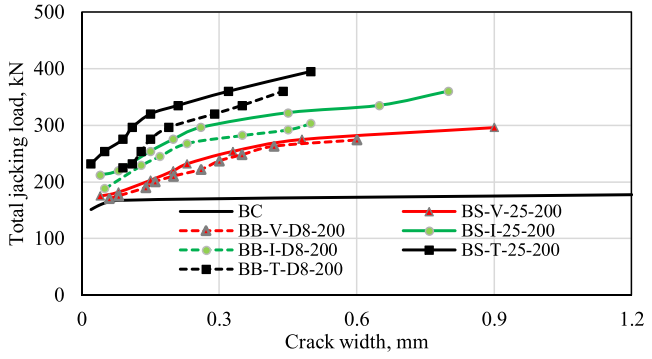


Fig. 20. Load versus shear crack width at the reinforced side for all beams of groups 2 and 3.

Fukuyama et al. [66] proposed a simple expression for estimating the average shear crack width (w_{av}) based on the effective depth of the concrete cross-section (d_e) and the developed strain on the shear reinforcement (ε_w) as given in Eq. (5).

$$w_{av} = 0.9 d_e \frac{\varepsilon_w}{\sqrt{2}} \tag{5}$$

Piyamahant [62] took into account the effect of shear reinforcement diameter (d_{by}), normalized slip of the shear reinforcement involving the shear reinforcement strain (ε_w) and the concrete cylinder compressive strength ($f_c^{'}$) as given in Eq. (6).

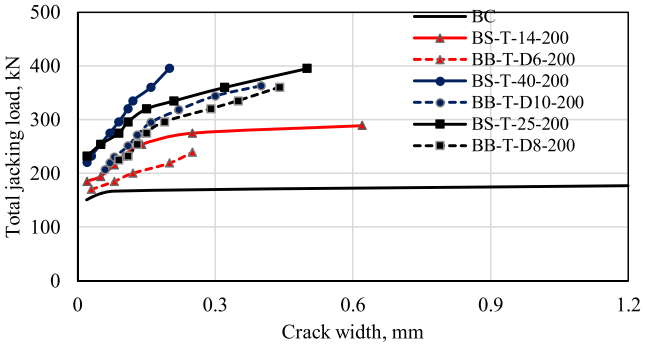


Fig. 21. Load versus shear crack width at the reinforced side for all beams of groups 4 and 5.

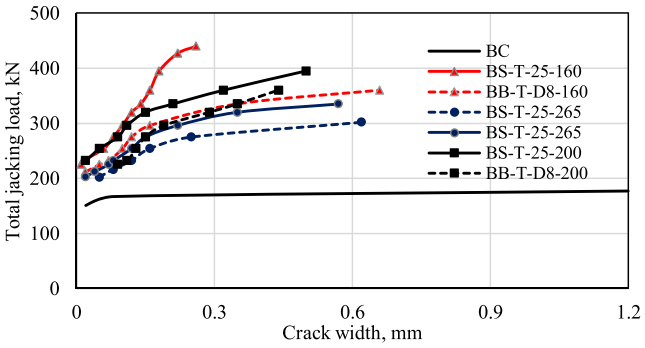


Fig. 22. Load versus shear crack width at the reinforced side for all beams of groups 6 and 7.

$$w_{av} = \frac{2 d_{by} \varepsilon_w (6 + 3500 \varepsilon_w)}{\left(\frac{f_c^{'}}{20}\right)^{2/3}} \tag{6}$$

Assuming linear relationship between shear crack width and stirrup strain, De Silva et al. [55] proposed that the average shear crack width (w_k) is equal to the product of the average spacing of shear cracks ($s_{m\theta}$) and the stirrup strain (ε_w) as given by Eq. (7).

$$w_k = k_w . s_{m\theta} . \varepsilon_w \tag{7}$$

Where k_w is a coefficient taking into account the inclination of the web reinforcement to the member axis = 1.2 for vertical stirrups; 0.8 for stirrups inclined with 45^0 to 60^0 and the average spacing of shear cracks $s_{m\theta}$ can be calculated by Eq. (8).

$$s_{m\theta} = \left[\frac{1}{\frac{\sin\theta}{s_{mx}} + \frac{\cos\theta}{s_{my}}} \right] \tag{8}$$

Where θ is the inclination angle of the shear crack with horizontal; s_{mx} and s_{my} are the horizontal and vertical crack spacing, respectively, as given by Eqs. (9) and (10).

$$s_{mx} = 2\alpha_1 \left[c_x + \frac{s_x}{10} \right] + k_1 k_2 \alpha_1 \frac{d_{bx}}{\rho_x} \tag{9}$$

$$s_{my} = 2\beta_1 \left[c_y + \frac{s_y}{10} \right] + k_1 k_2 \beta_1 \frac{d_{bv}}{\rho_v} \tag{10}$$

Where c_x is the distance from the horizontal center line of the concrete cross-section to longitudinal reinforcements; c_y is the distance from the center line of the concrete cross-section to the inner edge of vertical reinforcement; s_x is the spacing between longitudinal reinforcement; s_y is the spacing between web reinforcement; k_1 is the bond coefficient =

0.8 for smooth bars; k_2 is the stress distribution coefficient; d_{bx} is the diameter of longitudinal bars; d_{bv} is the diameter of web reinforcement; ρ_x is the longitudinal reinforcement ratio; ρ_v is the web reinforcement ratio; α_1 and β_1 are correlation factors equal to 0.36.

Based on regression analysis, Zakaria et al. [65] assumed Eq. (11) for estimating the average shear crack width.

$$w_{av} = 0.112 k_s k_t (c_s)^{0.05} \left(\frac{1}{\rho_w}\right)^{0.207} \left(\frac{1}{\rho_l}\right)^{0.252} (1.25 s_{m\theta}) \varepsilon_w \quad (11)$$

Where $k_s = 1$ for closed ordinary stirrups; $k_t = 1.2$ for smooth plain bars; c_s is side concrete cover for shear reinforcement; ρ_w is the web reinforcement ratio; ρ_l is the longitudinal reinforcement ratio; $s_{m\theta}$ the average spacing of shear cracks that can be calculated by Eqs. (8), (9) and (10); ε_w is stirrup strain.

It is worth mentioning that the proposed models did not state the load level corresponding to the proposed shear crack width, i.e., the proposed shear crack width is corresponding to 90% of the failure load of the beam, less or more the mentioned percentage or corresponding to failure load. In the current test, measuring of shear crack width was stopped approaching failure when the beam seemed to be near failure. However, the failure load was unknown at that stage. Therefore, after complete failure, the load level at the last measuring shear crack width was compared to the failure load for each beam as summarized in Table 6. It can be observed that the stopping load level was not the same. It ranged from 90% up to near 100% of the failure load.

Table 7 compares the results of the maximum shear crack widths against the estimated shear crack widths using the adopted five models. It can be observed that the adopted models showed conservative results for most beams, however, some beams showed un-conservative results. On contrary, the model proposed by De Silva et al. [55] showed conservative results for all beams. In spite that the main parameter adopted by both De Silva et al. [55] and Zakaria et al. [65] are almost the same, the proposed equation by Zakaria et al. [65] showed higher shear crack widths, thus four beams exhibited un-conservative results by significant margin. The equations proposed by Fukuyama et al. [66] and Piyamahant [62] are very simple in application; however, they missed many controlling parameters. In addition, both equations showed un-conservative results for some beams; however, they showed better results than that exhibited by Zakaria et al. [65]. The results presented by Hassan et al. [58] showed good estimation for shear crack width results except one beam where its result was slightly higher than the experimental results.

Obviously, the adopted models did not consider the effect of using steel strips instead of rounded bars as well as they deal with individual web reinforcement not assembled truss. Experimental results showed that using steel strips decrease the shear crack width compared to the corresponding equivalent rounded bars taking into account the cross-sectional area and spacing. Therefore, new correction factor less than unity have to be introduced to take into account such effect. Besides, the loading level corresponding to the estimated shear crack width has to be identified clearly. For this purpose, the shear crack widths for beams reinforced with trussed strips were estimated at the last measured load level of the corresponding beams reinforced with equivalent trussed bars as summarized in Table 6. Then the ratio between the crack widths for beams reinforced with trussed strips at such load level and the corresponding crack width exhibited by beams reinforced with equivalent trussed bars was calculation as mentioned in Table 6. The average value of the results of 7 beams was about 0.54, while the minimum and maximum values were 0.24 and 0.8, respectively. Accordingly, a reduction factor can be assumed for shear crack width ranged between 0.24 and 0.8, having an average value of about 0.54 can be assumed. Thus, additional tests have to be carried out to tackle such gap of knowledge in order to obtain a verified reduction factor, taking into account using either individual steel strips or trussed strips as web reinforcement.

4. Conclusion

The current paper proposed and implemented internal steel trusses made of either steel strips of 2 mm thickness or equivalent rounded steel bars assembled using welded connections in order to resist shear stress in reinforced concrete beams. Different alignment (vertical, inclined and combined vertical and inclined) of the truss members, different cross-sectional area of the truss members and different spacing have been investigated for both trussed strips and trussed bars. Based on the adopted concrete dimensions, material properties and the configurations of the used steel assemblies, shear span-to-depth ratio and the adopted incremental static loading, the following conclusions could be drawn:

1. Using internal steel configuration in the form of vertical strips, inclined strips and trussed strips enhanced the ultimate capacity of reinforced concrete beams by about 68%, 94% and 126%, as exhibited by beams BS-V-25-200, BS-I-25-200 and BS-T-25-20, respectively, compared to that of the control unreinforced beam BC. On the other hand, using equivalent trusses made of rounded steel bars resulted in decrease such enhancements to 52%, 66% and 96%, respectively, for beams BB-V-D8-200, BB-I-D8-200 and BB-T-D8-20.
2. It was found that, as expected, the ultimate capacity of trussed-reinforced beam is directly proportional to the cross-sectional area of the truss members and inversely proportional to the spacing

Table 6
Load level corresponding to measured maximum shear crack width for all reinforced beams.

Group No.	Specimen	w_{cr}(mm)	P_u (kN)	$P_{u,\ max\ cr}$(kN)	$P_{u,\ max\ cr}/P_u$	$w_{cr\ (bar)}$(mm)	$w_{cr\ (bar)}/w_{cr\ (eq)}$
2	BS-V-25-200	0.90	317.6	296	0.93	0.48	0.48/0.60 = 0.80
	BS-I-25-200	0.80	366.2	360	0.98	0.33	0.33/0.50 = 0.66
	BS-T-25-200	0.50	426.7	395	0.93	0.32	0.32/0.44 = 0.73
3	BB-V-D8-200	0.60	287.7	274	0.95	NA	
	BB-I-D8-200	0.50	314.2	303	0.96	NA	
	BB-T-D8-200	0.44	370.7	360	0.97	NA	
4	BS-T-14-200	0.62	289.3	289	1.00	0.12	0.12/0.25 = 0.48
	BS-T-40-200	0.20	437.0	395	0.90	0.16	0.16/0.40 = 0.40
5	BB-T-D6-200	0.25	240.4	239	0.99	NA	
	BB-T-D10-200	0.40	373.3	360	0.96	NA	
6	BS-T-25-160	0.25	454.9	440	0.97	0.16	0.16/0.66 = 0.24
	BS-T-25-265	0.57	364.0	335	0.92	0.27	0.27/0.62 = 0.44
7	BB-T-D8-160	0.66	386.2	360	0.93	NA	
	BB-T-D8-265	0.62	336.6	302	0.90	NA	

P_u = Failure load, $P_{u,\ max\ cr}$ = the load corresponding to the maximum measured shear crack width, w_{cr} = maximum measured shear crack width, $w_{cr\ (bar)}$ = the crack width for beams reinforced with steel truss at the corresponding final load of the beam reinforced with equivalent rounded bars, $w_{cr}(eq)$ = the corresponding crack width of the equivalent bar.

Table 7
Comparisons between experimental shear crack widths and the estimated shear crack widths using different proposed models.

Group No.	Specimen	Exp. mm(3)	Hassan et al. [58](4)	Fukuyama et al. [66](5)	Piyamahant [62](6)	De Silva et al.[55](7)	Zakaria et al. [65](8)	(3)/(4)	(3)/(5)	(3)/(6)	(3)/(7)	(3)/(8)
2	BS-V-25-200	0.90	0.37	0.30	0.23	0.36	0.53	2.41	3.00	3.94	2.50	1.69
	BS-I-25-200	0.80	0.38	0.30	0.23	0.26	0.60	2.13	2.67	3.50	3.04	1.33
	BS-T-25-200	0.50	0.14	0.30	0.23	0.20	0.40	3.62	1.67	2.19	2.44	1.25
3	BB-V-D8-200	0.60	0.43	0.33	0.27	0.40	0.59	1.39	1.79	2.24	1.51	1.02
	BB-I-D8-200	0.50	0.44	0.33	0.27	0.29	0.66	1.14	1.50	1.87	1.72	0.75
	BB-T-D8-200	0.44	0.16	0.33	0.27	0.22	0.43	2.74	1.32	1.65	1.99	1.02
4	BS-T-14-200	0.62	0.22	0.30	0.17	0.22	0.49	2.81	2.07	3.62	2.76	1.26
	BS-T-40-200	0.20	0.09	0.30	0.29	0.18	0.32	2.13	0.67	0.70	1.10	0.62
5	BB-T-D6-200	0.25	0.26	0.34	0.20	0.24	0.53	0.97	0.74	1.23	1.03	0.47
	BB-T-D10-200	0.40	0.11	0.33	0.32	0.20	0.35	3.70	1.22	1.24	2.02	1.14
6	BS-T-25-160	0.25	0.10	0.30	0.23	0.19	0.35	2.48	0.83	1.09	1.33	0.72
	BS-T-25-265	0.57	0.21	0.30	0.23	0.23	0.47	2.73	1.90	2.50	2.52	1.21
7	BB-T-D8-160	0.66	0.12	0.33	0.27	0.20	0.37	5.67	1.97	2.47	3.28	1.77
	BB-T-D8-265	0.62	0.24	0.33	0.27	0.27	0.56	2.56	1.85	2.32	2.31	1.11

between vertical members. However, the ultimate capacities for all beams reinforced with trussed strips were higher than those of beams reinforced with the corresponding trusses made of equivalent rounded bars.

3. In average sense, the ultimate capacity for reinforced concrete beams reinforced with internal steel trussed strips are higher than the corresponding capacity of equivalent trussed bars by about 16%.
4. Ant any load level, the flexural stiffness of the beam reinforced with trussed strips was higher than the corresponding stiffness demonstrated by the opponent beam reinforced with equivalent trussed bars.
5. Using steel strips to form the internal steel truss is better than using equivalent rounded steel bars where internal steel strips hindered the appearance of the shear cracking compared to the case of using steel truss formed from equivalent rounded steel bars.
6. The developed shear cracks were close to be perpendicular to the inclined members for the trussed strips. That can explain the reason for higher shear resistances of trussed strips than that developed by trussed bars.
7. For different configurations, cross-sectional area of the truss members and the spacing between vertical members, the developed shear crack width at any load level for beams reinforced with trussed strips was narrower than the developed shear crack width for the corresponding beams reinforced with equivalent trussed bars. The major shear cracks widths near failure were about 0.9, 0.8, 0.5, 0.6, 0.5, and 0.44 for beams reinforced with vertical strips, inclined strips, trussed strips, vertical bars, inclined bars, and trussed bars, respectively. It is worth mentioning that the measured shear crack widths were near failure for each beam, which was differed from one to another. Besides, the major shear crack widths near failure were about 0.62, 0.2, 0.25, and 0.40 for beams reinforced with trussed strips with 14 mm strip width, trussed strips with 40 mm strip width, trussed bars with 6 mm bar diameter, and trussed bars with 10 mm bar diameter. Furthermore, the major shear crack widths near failure were about 0.66, 0.62, 0.26, and 0.57 for beams reinforced with trussed strips with 160 mm strip spacing, trussed strips with 265 mm strip spacing, trussed bars with 160 mm bar spacing, and trussed bars with 265 mm bar spacing.
8. The load level corresponding to the maximum shear crack width is not fully defined in literature, which makes some discrepancy between the experimental results of the major shear crack width and the obtained analytical results based on the available models. In spite that the load levels percentage to failure load corresponding to measured shear crack width were dissimilar, the experimental results showed comparable results against the results of some available equations proposed for calculating the shear crack width. However, a new reduction factor taking into account the reinforcement type for steel strips either in individual or trussed form has to be introduced.

Declaration of Competing Interest

The authors declare that they have no known competing financial interests or personal relationships that could have appeared to influence the work reported in this paper.

References

[1] Lim DH, Oh BH. Experimental and theoretical investigation on the shear of steel fiber reinforced concrete beams. Eng Struct 1999;21(10):937–44.
[2] Park R, Paulay T, editors. Reinforced Concrete Structures. Wiley; 1975.
[3] Daou YA, Ghanem H. Study of the minimum shear reinforcement in high strength concrete Beams. Alexandria Eng J 2003;42(4):601–15.
[4] ASCE-ACI Committee 445. Recent approaches to shear design of structural concrete. 1998, 1375-1417.
[5] Ribas González CR, Fernández Ruiz M. Influence of flanges on the shear carrying capacity of reinforced concrete beams without web reinforcement. Struct Concr 2017;18(5):720–32.
[6] Zararis IP. Shear strength of reinforced concrete T-beams. ACI Struct J 2006;103:693–700.
[7] Choi K-K, Park H-G. Unified shear strength model for reinforced concrete beams - Part II: Verification and simplified method. ACI Struct J 2007;104(2):153–61.
[8] Wolf TS, Frosch RJ. Shear design of prestressed concrete: A unified approach. J Struct Eng 2007;133(11):1512–9.
[9] Muttoni A, Fernandez-Ruiz M. Shear strength of members without transverse reinforcement as function of critical shear crack width. ACI Struct J 2008;105(2):163–72.
[10] Colajanni P, Recupero A, Spinella N. Generalization of shear truss model to the case of SFRC beams with stirrups. Comp Concr 2012;9(3):227–44.

[11] Ferreira D, Bairán J, Marí A. Numerical simulation of shear-strengthened RC beams. Eng Struct 2013;46:359–74.
[12] Cladera A, Marí A, Bairán JM, Ribas C, Oller E, Duarte N. The compression chord capacity model for the shear design and assessment of reinforced and prestressed concrete beams. Struct Concr 2016;17(6):1017–32.
[13] Bairán JM, Marí A, Cladera A. Analysis of shear resisting actions by means of optimization of strut and tie models taking into account crack patterns. Hormigón y Acero 2018;69(286):197–206.
[14] Ashour SA, Hasanain GS, Wafa FF. Shear behavior of high-strength fiber reinforced concrete beams. ACI Struct J 1992;89(2):176–84.
[15] Kwak YK, Eberhard MO, Kim WS. Shear strength of steel fiber-reinforced concrete beams without stirrups. ACI Struct J 2002;99(4):530–8.
[16] Baby F, Marchand P, Toutlemonde F. Shear behavior of ultrahigh performance fiber-reinforced concrete beams. I: experimental investigation. J Struct Eng 2014; 140(5):04013111. https://doi.org/10.1061/(ASCE)ST.1943-541X.0000907.
[17] Parra-Montesinos GJ. Shear strength of beams with deformed steel fibers. Concr Int 2006;28(11):57–66.
[18] Hegger J, Bertram G. Shear carrying capacity of steel fiber reinforced UHPC. In: Ultra High Performance Concrete (UHPC): proceedings of the second international symposium on Ultra High Performance Concrete, Kassel, 5–7 March 2008, pp. 513-520. Kassel: Kassel University Press.
[19] Hussein L, Amleh L. Structural behavior of ultra-high performance fiber reinforced concrete-normal strength concrete or high strength concrete composite members. Constr Build Mater 2015;93:1105–16.
[20] Lampropoulos AP, Paschalis SA, Tsioulou OT, Dritsos SE. Strengthening of reinforced concrete beams using-ultra high performance fiber reinforced concrete (UHPFRC). Eng Struct 2016;106:370–84.
[21] Martinola G, Meda A, Plizzari GA, Rinaldi Z. Strengthening and repair of RC beams with fiber reinforced concrete. Cem Concr Compos 2010;32(9):731–9.
[22] Noshiravani T, Brühwiler E. Experimental investigation on reinforced ultra-high performance fiber reinforced concrete composite beams subjected to combined bending and shear. ACI Struct J 2013;110(2):251–61.
[23] Qi J, Wang J, Ma ZJ. Flexural response of high-strength steel-ultra-high-performance fiber reinforced concrete beams based on a mesoscale constitutive model: experiment and theory. Struct Concr 2018;19(3):719–34.
[24] Bahraq AA, Al-Osta MA, Ahmad S, Al-Zahrani MM, Al-Dulaijan SO, Rahman MK. Experimental and numerical investigation of shear behavior of RC beams strengthened by ultra-high performance concrete. Int J Concr Struct Mater 2019;13 (6):1–19.
[25] Yavaş A, Hasgul U, Turker K, Birol T. Effective fiber type investigation on the shear behavior of ultra-high-performance fiber-reinforced concrete beams. Adv Struct Eng 2019;22(7):1591–605.
[26] Al-Tersawy SH. Effect of fiber parameters and concrete strength on shear behavior of strengthened RC beams. Constr Build Mater 2013;44:15–24.
[27] Chaboki HR, Ghalehnovi M, Karimipour A, de Brito J, Khatibinia M. Shear behavior of concrete beams with recycled aggregate and steel fibers. Constr Build Mater 2019;204:809–27.
[28] Etman EE, Afefy HM, Baraghith AT, Khedr SA. Improving the shear performance of reinforced concrete beams made of recycled coarse aggregate. Constr Build Mater 2018;185:310–24.
[29] Wakjira TG, Ebead U. A shear design model for RC beams strengthened with fabric reinforced cementitious matrix. Eng Struct 2019;2001:109698.
[30] ACI Committee 318, Building Code Requirements for Structural Concrete (ACI 318M-18) and Commentary (ACI 318RM-18), American Concrete Institute (ACI), Farmington Hills, Michigan, 2018.
[31] Egyptian code for design and construction of reinforced concrete structures (ECP 203–2019); 2019.
[32] Abdul Hamid NA. The use of horizontal and inclined bars as shear reinforcement. MSc. Thesis, Faculty of Civil Engineering, University of Technology Malaysia 2005.
[33] Al-Nasra M, Asha N. The use of bolted u-Link swimmer bars in the reinforced concrete beams. International Organization of Scientific Research, J Eng (IOSRJEN) 2013;3(10):26–32.
[34] Al-Nasra M, Asha N. Investigating the use of spliced swimmer bars as shear reinforcement in reinforced concrete beams. International Organization of Scientific Research, J Eng (IOSRJEN) 2015;5(2):47–54.
[35] Al-Nasra M. The use of space swimmer bars as shear reinforcement in reinforced concrete beams. Int J Eng Technol (IJET) 2017;9(2):946–54.
[36] Ammash H. Behavior of reinforcement concrete beams using steel strips as a shear reinforcements. Int J Applied Eng Res 2017;12(19):8681–8.
[37] Shatarat N, Katkhuda H, Abdel-Jaber M, Alqam M. Experimental investigation of reinforced concrete beams with spiral reinforcement in shear. Constr Build Mater 2016;125:585–94.
[38] Zhang N, Fu C, Chen L, He L. Experimental studies of reinforced concrete beams using embedded steel trusses. ACI Struct J 2016;113(4):701–10.
[39] Adhikary BB, Mutsuyoshi H. Shear strengthening of reinforced concrete beams using various techniques. Constr Build Mater 2006;20(6):366–73.
[40] Campione G, Colajanni P, Monaco A. Analytical evaluation of steel-concrete composite trussed beam shear capacity. Mater Struct 2016;49(8):3159–76.
[41] Monaco A. Experimental analysis, numerical and analytical modeling of shear strength mechanisms in hybrid steel trussed concrete beams. Ph.D. Thesis, Universita' degli Studi di Palermo, Palermo, PA, Italy, 2014.
[42] Quaranta G, Petrone F, Marano G, Monti G. Structural design of composite concrete-steel beams with spatial truss reinforcement elements. Asian J Civil Eng (Building and Housing) 2011;12(2):155–78.
[43] Tesser L, Scotta R. Flexural and shear capacity of composite steel truss and concrete beams with inferior precast concrete base. Eng Struct 2013;49:135–45.
[44] Zhang W, Huang Z, Fu Z, Qian X, Zhou Y, Sui L. Shear resistance behavior of partially composite Steel-Concrete-Steel sandwich beams considering bond-slip effect. Eng Struct 2020;210:110394. https://doi.org/10.1016/j.engstruct.2020.110394.
[45] EN 1994-1-1: Eurocode 4: Design of composite steel and concrete structures – Part 1-1: General rules and rules for buildings. 2005.
[46] Petrone F. Shear resisting mechanisms in ccomposite steel-concrete beams. Department of Structural and Geotechnical Engineering. Italy: Sapienza University of Rome; 2012.
[47] Trentadue F, Quaranta G, Carlo Marano G, Monti G. Simplified lateral-torsional buckling analysis in special truss reinforced composite steel-concrete beams. J Struct Eng 2011;137(12):1419–27.
[48] Chisari C, Amadio C. An experimental, numerical and analytical study of hybrid RC-encased steel joist beams subjected to shear. Eng Struct 2014;61:84–98.
[49] Colajanni P, La Mendola L, Latour M, Monaco A, Rizzano G. FEM analysis of push-out test response of hybrid steel trussed concrete beams (HSTCBs). J Constr Steel Res 2015;111:88–102.
[50] Arafa M, Alqedra MA, Salim R. Performance of RC beams with embedded steel trusses using nonlinear FEM analysis. Adv Civil Eng 2018; Article ID 9079818: 1-8.
[51] Tullini N, Minghini F. Nonlinear analysis of composite beams with concrete-encased steel truss. J Constr Steel Res 2013;91:1–13.
[52] Gendron G, Picard A, Guérin M-C. A theoretical study on shear strengthening of reinforced concrete beams using composite plates. Compos Struct 1999;45(4): 303–9.
[53] Adebar P, Leeuwen JV. Side-face reinforcement for flexural and diagonal cracking in large concrete beams. ACI Struct J 1999;96(5):693–704.
[54] Zararis PD. Shear strength and minimum shear reinforcement of RC slender beams. ACI Struct J 2003;100:203–14.
[55] De Silva S, Mutsuyoshi H, Witchukreangkrai E. Evaluation of shear crack width in I-shaped prestressed reinforced concrete beams. J Adv Concr Technol 2008;6(3): 443–58.
[56] Hassan HM, Ueda T, Tamai S, Okamura H. Fatigue test of reinforced concrete beams with various types of shear reinforcement. Transaction of JCI 1985;7: 277–84.
[57] Hassan HM, Ueda T. Relative displacement along shear crack of reinforced concrete beam. Proceedings of JCI 1987;9(2):699–704.
[58] HASSAN HM, FARGHALY SA, UEDA T. Displacements at shear crack in beams with shear reinforcement under static and fatigue loadings. Concrete Library of JSCE 1991;(433):215–22. https://doi.org/10.2208/jscej.1991.433_215.
[59] Hassan HM. Shear cracking behavior and shear resisting mechanism of reinforced concrete beams with web reinforcement. PhD. Thesis. Japan: University of Tokyo; 1987.
[60] Witchukreangkrai E, Mutsuyoshi H, Takagi M, De Silva S. Evaluation of shear crack width in partially prestressed concrete members. Proceedings of JCI 2006;28(2): 823–8.
[61] Rizkalla SH, Hwang LS, El Shahawai M. Transverse reinforcement effect on cracking behavior of RC members. Canadian J Civil Eng 1983;10(4):566–81.
[62] Piyamahant S. Shear behavior of reinforced concrete beams with a small amount of web reinforcement. M. Eng. Dissertation. Kochi University of Technology, Japan, 2002.
[63] Shioya T, Iguro M, Nojiri Y, Akiyama H, Okada T. Shear strength of large reinforced concrete beams. Fracture Mechanics: Application to Concrete, SP 118, American Concrete Institute, Detroit, 309. 1989.
[64] Sherwood EG, Bentz EC, Collins MP. Effect of aggregate size on beam-shear strength of thick slabs. ACI Struct J 2007;104(2):180–90.
[65] Zakaria M, Ueda T, WE Z. Evaluating and proposing prediction models for shear crack width in concrete beams. J Japan Society Civil Eng, (Mater Concr Struct) 2011;67(2):245–63.
[66] Fukuyama H, Suwada H, Iso M, Matsuzaki Y, Nakano K, Kasahara M. Evaluation of damage limit state of RC element due to shear crack width. Proceedings of Architectural Institute of Japan (AIJ), (C-2) 2000, 13-14. (In Japanese).